Ricardo Jorge Segurado Lampreia

Licenciado em Ciências da Engenharia Electrotécnica e de Computadores

QoS in LEO Satellite Networks with Multipacket Reception

Dissertação apresentada para obtenção do Grau de Mestre em Engenharia Electrotécnica e de Computadores, pela Universidade Nova de Lisboa, Faculdade de Ciências e Tecnologia.

Orientadores : Luís Bernardo, Professor Auxiliar com Agregação, FCT-UNL

Rui Dinis, Professor Auxiliar com Agregação, FCT-UNL

Júri:

Presidente: Prof. Doutor Pedro Amaral

Arguentes: Prof. Doutora Teresa Vasques

Vogais: Prof. Doutor Luís Bernardo

Prof. Doutor Rui Dinis

FACULDADE DE CIÊNCIAS E TECNOLOGIA
UNIVERSIDADE NOVA DE LISBOA

Setembro 2013

QoS in LEO Satellite Networks with Multipacket Reception

"The only source of knowledge is experience."

Albert Einstein

To my parents and friends.

Agradecimentos

Quero começar por agradecer ao meu orientador, o Professor Luís Bernardo, pela amizade, dedicação, disponibilidade e paciência demonstrada ao durante todos os momentos desta dissertação. Foi sem dúvida uma orientação de excelência. Agradeço ao coorientador Rui Dinis, pela disponibilidade prestada. E também queria deixar uma palavra de homenagem à memória do coorientador, Professor Mário Macedo, obrigado por tudo.

Agradeço aos meus colegas de laboratório José Vieira, Pedro Cunha, Fábio Júlio, Bruno Branco, Miguel Duarte, Luís Irio, João Chalaça e Bruno Domingos pela amizade e pelo incrível espirito de camaradagem.

A todos os colegas que fizeram parte do meu percurso universitário, nomeadamente, Joana Martelo, Franscisco Esteves, Pedro Almeida, Pedro Vilaça, André Rocha, Gonçalo Alves, Rui Borrego, Patrick Boura, Rúben Galante, João Filipe, Tiago Conraria, Ricardo Silva e Ricardo Ferreira, levo a vossa amizade por muitos e bons anos.

Quero agradecer aos meus amigos fora do curso, Emanuel Ferreira, Joaquim Conde, Pedro Ribeiro, Vera Rocha, Sónia Silva, José Martins, Liliana Teodósio, Renata Cartaxo, Filipa Cristina e Fábio Oliveira pelo constante apoio.

Aos meus pais, Maria e José, pelo carinho, motivação e apoio demonstrado ao longo da minha vida. Fizeram sempre o maior esforço para que eu tivesse sucesso. E um obrigado ao resto da minha família.

Um agradecimento especial aos projectos da FCT/MEC: MPSat - PTDC/EEA-TEL/099074/2008, OPPORTUNISTIC CR - PTDC/EEA-TEL/115981/2009, Femtocells - PTDC/EEA-TEL/120666/2010 e ADIN - PTDC/EEI-TEL/2990/2012, pelo apoio financeiro e também pelo equipamento disponibilizado.

Resumo

As redes de satélite de baixa altitude (LEO), podem optimizar as redes sem fios terrestres, para fornecer serviços de banda larga aos terminais móveis (MT), numa escala global. Neste enquadramento, os sistemas de telecomunicações híbridos com componente de satélite e LTE, como o *LightSquared*, prometem oferecer serviços de alto débito ubíquos.

Neste trabalho é realizada uma análise ao desempenho de um protocolo de acesso aleatório, que aplica Hybrid Network-assisted Diversity Multiple Access (H-NDMA) a uma rede de satélites LEO, sendo denominado de Satellite Random NDMA (SR-NDMA). Para além disto, o desempenho do sistema é avaliado considerando para a transmissão ascendente, uma arquitectura Single Carrier-Frequency Domain Equalization (SC-FDE) e também um receptor Multipacket Recepetion (MPR).

Na primeira parte deste trabalho é implementado um simulador SR-NDMA para medir o desempenho do sistema, com base em taxas de débito, consumo de energia, atrasos e requisitos de qualidade de serviço (QoS). Para tal, são realizados vários testes com um gerador de tráfego aleatório, baseado numa distribuição de Poisson, com o intuito de validar o modelo analítico existente. Também são feitos testes com um módulo de geração de tráfego de tempo real, e é verificado se os requisitos de QoS são cumpridos.

Palavras Chave: QoS, Simulador SR-NDMA, Satélite LEO, SC-FDE, MPR, Acesso Aleatório

Abstract

Low Earth Orbit (LEO) satellite networks can improve terrestrial wireless networks to allow global broadband services for Mobile Terminals (MT), regardless of the users' location. In this context, hybrid telecommunication systems combining satellites with Long Term Evolution (LTE) networks, like the LightSquared technology, are intended to provide ubiquitous high-speed services.

This dissertation analyses the performance of a random access protocol that uses Hybrid Network-assisted Diversity Multiple Access (H-NDMA), for a LEO satellite system network, named by Satellite Random NDMA (SR-NDMA). The protocol also considers a Single Carrier-Frequency Domain Equalization (SC-FDE) scheme for the uplink transmission and a Multipacket Reception (MPR) receiver. In this scenario, the transmission of data packets between MTs and the Base Station (BS) is made through random access and schedule access slots, organized into super-frames with the duration of a Round Trip Time (RTT).

A SR-NDMA simulator is implemented to measure the system performance in matters of throughput, energy consumption, system delay and also the protocol capacity to meet Quality of Service (QoS) requirements. A set of simulations tests were made with a random Poisson process traffic generation to validate the analytical model. The capacity to fulfil the QoS requirements of a real-time traffic class was also tested.

Keywords: QoS, SR-NDMA Simualtor, LEO Satellite, SC-FDE, MPR, Random Access

Acronyms

3GPP *Third Generation Partnership Project*

ARQ *Automatic Repeat reQuest*

BER *Bit Error Rate*

BS *Base Station*

CBR *Constant Bit Rate*

CDMA *Code Division Multiple Access*

CoS *Classe of Service*

CPI *Cyclic Prefix Insertion*

DAMA *Demand Assignment Multiple Access*

DS-CDMA *Direct Sequence Code Division Multiple Access*

EPUP *Energy Per Useful Packet*

FDE *Frequency Domain Equalization*

FEC *Forward Error Correction*

FDM *Frequency Division Multiplexing*

FDMA *Frequency Domain Multiple Access*

FFT *Fast Fourier Transform*

GPD *Generalized Pareto Distribution*

GSM *Global System for Mobile Communications*

GSO *Geostationary Orbit*

HTTP *HyperText Transfer Protocol*

H-NDMA *Hybrid-ARQ NDMA*

IB-DFE *Iterative Block Decision-Feedback Equalizer*

IC *Multi-stage Interference Cancellation*

ID *User Identification*

IEEE *Institute of Electrical and Electronics Engineers*

IETF *Internet Engineering Task Force*

IFFT *Inverse Fast Fourier Transform*

IPDV *IP Packet Delay Variation*

IPER *IP Packet Error Ratio*

IPLR *IP Packet Loss Ratio*

IPTD *IP packet Transfer Delay*

ISI *InterSymbol Interference*

ISL *InterSatellite Links*

ITU-T *International Telecommunication Union- Telecommunication*

LANs *Local Area Networks*

LDPC *Low Density Parity Check*

LEO *Low Earth Orbit*

LTE *Long Term Evolution*

MAC *Medium Access Control*

MEO *Medium Earth Orbit*

MIME *Multipurpose Internet Mail Extensions*

MIMO *Multiple Input Multiple Output*

MMSE *Minimum Mean Square Error*

MPR *Multipacket Reception*

MT *Mobile Terminal*

MUD *Multi-User Detection*

NDMA *Network-assisted Diversity Multiple Access*

NGSO *Non-Geostationary Orbit*

NP *Network Performance*

OFDM *Orthogonal Frequency Division Multiplexing*

OSI *Open Systems Interconnection*

PAPR *Peak-to-Average Power Ratio*

PER *Packet Error Rate*

PIC *Parallel Interference Cancellation*

PSK *Phase Shift Keying*

PSTN *Public Switched Telephone Network*

QAM *Quadrature Amplitude Modulation*

QoS *Quality of Service*

RA *Random Access*

RSSI *Radio Signal Strength Indicator*

RSVP *Resource Reservation Protocol*

RTP *Real-time Transportation Protocol*

RTT *Round Trip Time*

R-ALOHA *Reservation Aloha*

R-TDMA *Request-TDMA*

SA *Schedule Access*

SC-FDE *Single Carrier-Frequency Domain Equalization*

SIC *Successively Interference Cancellation*

SIP *Session Initial Protocol*

SISO *Single-Input Single-Output*

SLA *Service Level Agreement*

SMS *Short Message Service*

SNR *Signal to Noise Ratio*

SR-NDMA *Satellite Random Network-assisted Diversity Multiple Access*

SYNC *Synchronization Signal*

S-NDMA *Satellite-NDMA*

TDMA *Time Division Multiple Access*

UDP *Used Datagram Protocol*

UHF *Ultra High Frequency*

UMTS *Universal Mobile Telecommunication System*

VAD *Voice Activation Detection*

VBR *Variable Bit Rate*

VHF *Very High Frequency*

VoIP *Voice over IP*

WANs *Wide Area Networks*

WLAN *Wireless Local Area Network*

Contents

List of Figures

List of Tables

List of Symbols

B_{max}	Maximum number of slots allocated by the satellite to a MT per RTT
$C_{p_{i,k}}$	Total number of packet copies
E_b	Average bit energy associated to a given packet transmission
$F_{k,p}$	Feed-forward coefficients of the linear receiver
$F_{\xi,\mu,\sigma}$	GPD cumulative distribution function
$H_{k,p}^{(r)}$	Channel frequency response from the pth user, during the rth transmission
J	Number of members of a group of MTs associated with a satellite
K_k^l	One number of MTs that successfully transmit at retransmission k during an SR-NDMA epoch with l retransmission super-slots
L_s	Saturation level
L_T	The total load injected into the system
l	lth transmission in a epoch
N	Maximum number of packets that a MT can send per epoch
N_0	Power spectral density of the noise
$N_k^{(r)}$	The channel noise during the rth transmission
N_s	Number of symbols in a data block

$\mathbf{n}^{(P)}$	Matrix containing all slots values, for all possible retransmissions, to be used for all possible P MTs
$\mathbf{n}^{(P)^\star}$	Optimal matrix containing all slots values, for all possible retransmissions, to be used for all possible P MTs
n_0	Number of random access slots used in the initial transmission
n_l	Number of slots used for the l transmission
n_R	Number of random access slots used in the last transmission
P	Number of transmitting users
Q_x	Gaussian error function
R	Scheduled retransmissions
$S_{k,p}$	Data block transmitted by a user p, in the frequency domain
$S_{p_{i,k}}$	Total amount of successful received packets in a specific RTT cycle by a given MT
$s_{k,p}$	Data block transmitted by a user p, in the time domain
T	Round Trip Time in slots
T_{RTT}	Maximum interval of RTT simulation cycles
S	Throughput
U	Uniformly distributed variable
X	Number of events which happen in a time unit
$x_{i,k}$	The total amount of successful packets sent by a station in a specific RTT cycle
x_i	Matrix representing the slots where the MTs transmitted until the current super-frame during the transmission epoch
$Y_k^{(r)}$	Received signal, from multiple MTs, at the receiver in the frequency domain for a given transmission r

ϵ	Packet loss ratio
λ	Average packet generation rate per MT
$\lambda_{i,k}$	Generated load in every RTT cycle
Ω_p^l	The space state defined by the SR-NDMA epoch with l retransmission super-slots and P MTs
$\Psi^{P,R}$	Random state vector that defines the packet transmission behaviour
$\psi_l^{P,l}$	The random state vector with the number of MTs that successfully transmit at retransmission
ρ	Load factor
τ_{max}	Maximum delay value
σ_j	Jitter
τ_T	Sum of every successful packet delay in a given T_{RTT} interval
$\zeta_l^{(P)}$	Total number of slots for P users until the lth transmission

Chapter 1

Introduction

The Introduction chapter gives a first presentation of this work, with the motivation behind the dissertation subject, the main objectives and contributions, followed by the description of the work structure.

1.1 Motivation

Since the time that the satellite communications systems were primarily considered for naval and aeronautical purposes, to nowadays, that there was a continuous evolution which led to the integration of satellite systems in terrestrial telecommunications services. This integration can allow the telecommunication networks to provide wireless networks in a simpler, faster and more reliable way everywhere, at any time. As an example of this applicability, it is possible to guarantee the communication during natural disasters and emergencies when the terrestrial infrastructure is down.

With the constant urge to have better wireless broadband internet in Mobile Terminals (MTs) with guarantees of Quality of Service (QoS) and full connectivity, it is of interest to have the integration of terrestrial and satellite communication networks. In this context, hybrid telecommunication systems combining satellites with Long Term Evolution (LTE) networks, like the LightSquared technology, are envisioned to provide ubiquitous high-speed services.

The main obstacles in the integration of both networks, are related to the higher satellite propagation delays and the higher transmission requirements, inherent to the

distance of the satellite to the MT. On the other hand, the MTs must have low cost and be efficient in terms of energy consumption.

1.2 Objectives and Contributions

The objectives for this thesis are the development of a Satellite Random Network-assisted Diversity Multiple Access (SR-NDMA) protocol system [VGaB+13] simulator with multimedia traffic generator modules and the subsequent performance analysis.

Initially, a scenario composed by a Low Earth Orbit (LEO) satellite network is considered, based on the Iridium satellite constellation, using Single Carrier-Frequency Domain Equalization (SC-FDE) scheme for the uplink transmission and Multipacket Reception (MPR). In this scenario, the transmission of data packets between MTs and the Base Station (BS) is made through random access and schedule access slots, organized in superframes with the duration of a Round Trip Time (RTT).

A random exponential traffic generator (an approximation of the Poisson load generator) is used to validate the SR-NDMA Medium Access Control (MAC) analytical model. The performance analysis is based on throughput, energy consumption, delay and jitter measurements.

In the second part of this thesis, the SR-NDMA simulator performance is used to evaluate if the QoS requirements of a real-time traffic class are satisfied. For this, an audio traffic class generator module is applied, composed by random time intervals of call arrivals/on hold and speech patterns. Also, it is created a module to generate the codec *ON* and *OFF* periods, to allow the packet injection into the waiting queue.

This work contributed to provide:

- a simulation testing environment for the SR-NDMA protocol with several configurable parameters.

- models for real-time traffic, which can not be analytically translated due to the complexity of the mathematical models associated.

1.3 Dissertation Structure

This dissertation is briefly described as follows: Chapter 2 refers the current state of the art with an overview on the satellite networks and the used multiple access schemes, error control mechanisms, MAC protocols, collision resolution methods and finalizing with a brief overview about QoS.

Chapter 3 presents the SR-NDMA protocol description, an explanation about the traffic generation considered for the simulator and the measurements of the system performance.

The SR-NDMA simulator development and the support of QoS data sources is presented in Chapter 4. The respective results from the simulator are analysed in Chapter 5.

Finally, in Chapter 6, final conclusions of all the development and a plan for future works are given.

Chapter 2

Related Work

This chapter comprehends the state of the art study regarding: the satellite system considered for this thesis, schemes for multiple access, several MAC protocols, the interaction between different types of layers and Quality of Service aspects.

2.1 Satellite Constellations

A satellite system can have two types of constellations: Geostationary Orbit (GSO) or Non-Geostationary Orbit (NGSO).

The geostationary terminology is applied when satellites present a circular motion around Earth, approximately, in twenty-four hours. This means that the motion is synchronized with the planet movement. With an altitude of 35786 km from the equator line, each GSO satellite can cover about one-third of the Earth's surface, so the full coverage (not considering the Polar Regions) is achieved with a small constellation. The altitude of the satellite also has disadvantages for this kind of constellation, since it takes large antennas and a high transmit power to mitigate signal degradation. It is also necessary to consider the propagation delay of about 250 ms, which is not suitable for real-time traffic [HL01].

Regarding the NGSO satellite systems, they present a satellite asynchronous movement in relation to the Earth rotation, combined with two zones of distinct orbits: LEO which is located at an altitude between 500 to 2000 km from the Earth's surface, and Medium Earth Orbit (MEO) from 8000 to 12000 km [BWZ00]. NGSO satellites have, in

relation to the GSO, lower power requirements, and less propagation delay due to its altitude. Although the altitude makes it also necessary to have more satellites in the satellite network; some examples of current LEO satellite networks operating have 12, 24 and 66 (or more) satellites for global coverage (covering the polar regions contrarily to the GSO satellite networks) [Ipp08].

2.1.1 LEO Satellite Systems

LEO satellites can be used in certain sceneries which require low delay and low bit error characteristics [NBSL11]. Due to its low altitude, the LEO satellites must be served by a big number of earth stations to maintain transmission, that can be in some cases about 200 or more, and considering as well the risk of "shadowing" of the signal by vegetation, terrain and buildings [Man95].

There are three types of systems that are differentiated in matters of main applications offered by the satellite. The first type is named Little LEO and is for low bit rate data applications, given by, for example, the ORBCOMM system [Maz99]. This system provides electronic mail and paging to mobile devices. The second system (Big LEO) is used for mobile telephony applications, like providing narrow-band mobile voice services. Iridium and Globalstar are examples of this kind of system. Finally, Broadband LEO offers high bit rate data, which provides primarily fixed, broadband connections comparable to urban wireline service [Uni02].

2.1.2 Iridium Satellite System

Motorola's Iridium system was chosen to be the base of research for this thesis. It was conceived in 1987, based on a constellation proposed by Adams and Rider [AR87], intending to be the first private global wireless communication system to provide a wide diversity of services such as voice, data, fax and paging. In May 1998, the system was completely deployed as a constellations of 66 cross-linked (plus seven in-orbit spares), divided in groups of 11 satellites per plane, with a spacing of 32 degrees of latitude.

Due to satellite movement or the mobility of the user, it is necessary to transmit the signal to another satellite or a gateway on ground. So the Iridium system uses Inter-

Satellite Links (ISL) to route traffic, while the regional gateways will handle call setup procedures and interface IRIDIUM with the existing public switched telephone network (PSTN). Iridium provides a network where the satellites communicate with other satellites that are near and in adjacent orbits. This kind of operation allows a simple call to roam over several satellites, coming back to the ground when downlinked at an Iridium gateway, and patched into a PSTN for subsequent transmission to destination. Each satellite has on Earth's surface 48 spot beams, with 402 Km of diameter apiece, to decrease the probability of existing dropped calls or missed connections.

Communication between satellites and handsets is done in the Iridium system using L-band spectrum, between 1616 and 1626.5 MHz. But other frequency bands can be considered. Ultra High Frequency (UHF) and Very High Frequency (VHF) ranges (137 to 401 MHz) are commonly used by small LEO systems to provide low data rate transmissions, but none of them is appropriated for multimedia transmission. Higher data rates are available in the Ku (10 to 18 GHz), which are used to provide data communications to the subscriber, and Ka bands (18 to 31 GHz) to support communication between the satellite and the ground stations and between satellites [PRFT99].

The most important band frequencies, in relation to this thesis, which focuses the communication between the satellite and the user terminals, are the L band (1610 to 1626.5 MHz) and S band (2483.5 to 2500 MHz), which are generally used by LEO systems for telephone and Short Message Service (SMS) [BWZ00].

2.2 Multiple Access Schemes in Satellite Systems

In a multiple accessed channel, two or more users may nominally share the channel. The satellite system can provide broadcast capability at any given time to all earth stations within its transmission coverage area [Ret80]. There are several techniques that could support this capability. The most common are Code Division Multiple Access (CDMA), Frequency Domain Multiple Access (FDMA) and Time Division Multiple Access (TDMA). In more recent years, the pre-4G Third Generation Partnership Project (3GPP) LTE system has adopted two additional solutions: Orthogonal Frequency Division Multiplexing (OFDM) and SC-FDE.

2.2.1 Code Division Multiple Access

CDMA allows each terminal to transmit continuously and together on the same frequency spectrum given by the satellite. To distinguish a terminal in a simultaneous transmission, each one has its own pseudo-random code word which is approximately orthogonal to everyone else. The receiver must know all code words in advance, in order to perform a time operation correlation to detect the specific code word of a desired terminal. The operation is made without any awareness of a terminal in relation to others [Rap01]. This is referred to the Direct Sequence CDMA (DS-CDMA) modulation, which is used in almost all 3G mobile cellular systems as their prime multiple access air-link architecture [AG11].

CDMA can offer several advantages by its approach of including every transmission in a unique signal. A set of CDMA networks can share the same frequency band, by the fact that the undetected signal behaves as Gaussian noise to all receivers without knowledge of the code sequence, giving them also protection and privacy. Because only a small portion of the signal energy is present in a given frequency band segment at any time, the CDMA can provide jamming resistance created by the presence of undesirable signals in the frequency band, and reducing the effects of multipath fading [Ipp08].

But the power of multiple terminals at a receiver can give performance issues to a CDMA network. The power determines the noise floor after decorrelation. If each terminal power is not controlled, the receiver will get different levels of power. This is known as the near-far problem. The near-far problem occurs when a stronger received signal imposes a higher noise level in the demodulaters for weaker signals, decreasing the probability of a successful transmission. In order to resolve the near-far problem, in each base station is implemented a power control operation. The satellite samples the radio signal strength indicator (RSSI) of each terminal linked to him, and then sends a power change command to the higher power terminals. This operation can only reduce or raise interferences caused by the terminals inside the same cell [Rap01].

2.2.2 Frequency Domain Multiple Access

FDMA divides the frequency spectrum in channels, where each channel can allocate a single terminal and is possible to transmit simultaneously and continuously in multiple

channels. The allocation can be made on demand to terminals that have announced their intention to request a channel. When a terminal is transmitting or receiving (a channel has one frequency to uplink and another to downlink), the frequency band cannot be shared to another terminals. If a channel is not in use, then it turns to an idle state and it is impossible to be used by other terminals [Rap01].

Also the FDMA presents some limitations in large bandwidth scenarios, due to equalization complexity. FDMA was improved by two additional approaches: OFDM and SC-FDE.

2.2.2.1 Orthogonal Frequency Division Multiplexing

The OFDM technique is an evolution of Frequency Division Multiplexing (FDM), where several sub-carriers are transmitted in parallel and each one occupies a very narrow bandwidth. The transmission of the sub-carriers is modulated with Quadrature Amplitude Modulation (QAM) or Phase Shift Keying (PSK) at a lower transmission rate than the original signal. This allows a much more efficient struggle against multipath fading [PA02].

In figure 2.1, Inverse Fast Fourier Transform (IFFT) is applied on blocks of M data symbols at the transmitter side to generate the multiple sub-carriers. After this, it is inserted a cyclic prefix (CPI) to carry the repetition of the last symbol, in order to avoid InterSymbol Interference (ISI) with the previous block and make the received block look periodic, simulating a circular convolution and allowing an efficient FFT operation.

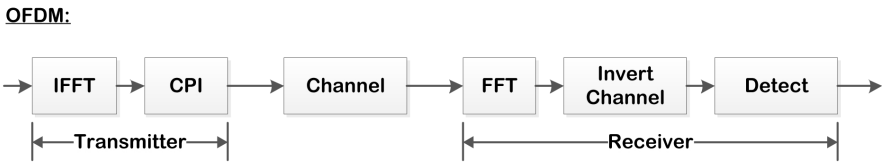

Figure 2.1: OFDM signal processing [FABSE02].

The sub-carriers are extracted in the receiver by applying a Fast Fourier Transform (FFT) on the received blocks. The cyclic prefix inserted previously in the block is also discarded.

OFDM signal is composed by the sum of several slowly modulated sub-carriers, resulting in a high peak-to-average power ratio (PAPR). The problem of these high peaks is most severe at the transmitter output. The transmission power of the amplifier must be reduced in some dB's, in order to maintain the linearity over the range of signal enve-

lope peaks that should be reproduced. But this solution also as a disadvantage, because the increased power back-off will raise the cost of the power amplifier and also the power consumption [FABSE02].

OFDM is used, for example, in the Institute of Electrical and Electronics Engineers (IEEE) 802.11 and 802.16 standards, and in the LTE and LTE Advanced [BS04].

2.2.2.2 Single Carrier - Frequency Domain Equalization

SC-FDE is an alternative to OFDM, where it is applied frequency domain equalization to a single carrier. This technique has some of the OFDM advantages as well, such as performance, efficiency and low signal processing complexity. The usage of a single carrier in SC-FDE decreases the PAPR. Therefore, the power amplifier of an SC transmitter does not need a big linear range to support a given average power, which represents a lower complexity of the power amplifiers. Also results in more efficient power consumption due to the reduced power back-off.

In figure 2.2, it is possible to see that the main difference of OFDM and SC-FDE is the placement of the IFFT block from the transmitter to the receiver side. This allows the conversion of Frequency Domain Equalization (FDE) signals into time domain symbols [FABSE02].

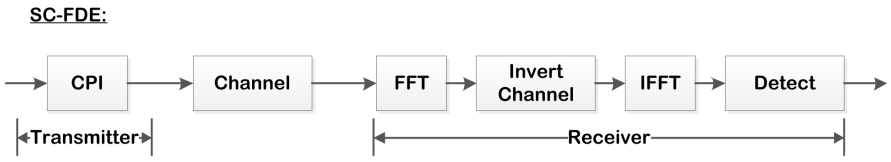

Figure 2.2: SC-FDE signal processing [FABSE02].

It is possible the coexistence of both systems, like for instances, in 3GPP LTE, SC-FDE is used in the uplink, and OFDM used in the downlink, avoiding IFFT operation complexity on the transmitter side, improving the terminal battery resources [BS04].

2.2.3 Time Division Multiple Access

In TDMA, the radio spectrum is divided into time slots, and only one terminal can transmit or receive in a time slot. The data packets are transmitted in bursts, thus the transmission of any terminal is non-continuous. This allows a much simpler handoff process to the

terminal, since they can listen for other base stations during idle time slots [Ipp08].

However, the TDMA requires a high synchronization overhead to guarantee synchronization between terminals and the correspondent data bursts. Also, it is usually necessary to have adaptive equalization to mitigate the effects of multipath propagation caused by very high transmission rates.

The TDMA was used in the Second Generation cellular systems like the Global System for Mobile Communications (GSM), but continues to be used mixed with other approaches (e.g. TDD OFDMA).

2.3 Error Correction Schemes

In a wireless communication channel transmission errors may occur due to several factors, like for instance, multipath fading. In order to detect and correct these errors, techniques such as Forward Error Correction (FEC) and Diversity Techniques are used.

2.3.1 Forward Error Correction

FEC techniques include redundant information inside each data block sent, which allows the receiver to know if the data block is successfully received, and in case of failure, what was the error. This technique differs from error-detecting codes, since they include only the necessary redundant information for the receiver to know that an error exists, but without knowing what the error is [AS02].

Turbo codes and Low Density Parity Check (LDPC) are the last generation of FEC techniques. They were created to resolve the issues of compatibility with FEC frame structures in some systems and to improve the coding gain [CF07]. FEC is commonly used in satellite communications since it provides the most powerful performance, and almost achieves the Shannon's theoretical limit. In 1948, Claude Shannon showed that for a given channel capacity there is a maximum data rate which allows data transmission with a small error probability. If the rate is higher than the channel capacity, there is no reliable FEC scheme [Sha48].

2.3.2 Diversity Techniques

To improve the performance in deep fade channels, it is necessary to ensure that the message signal passes through multiple signal paths. The combination of multiple versions of the original signal makes a new improved signal capable of mitigating the fading effects and channel interferences.

There are several ways to obtain diversity: over time, over frequency and over spatial domain. In time diversity, when a MT sends a data symbol with errors, the BS requests more retransmissions in different periods of time. Examples of this approach are the Automatic Repeat reQuest (ARQ) and Hybrid-ARQ schemes.

Frequency diversity uses several frequency channels to transmit the replicas of a data symbol. Since it tries to transmit data symbols more frequently, issues like ISI can appear. The frequency diversity deals with this problem in three different ways: Single-carrier systems with equalization, direct-sequence spread spectrum and OFDM.

In space diversity, the transmission signal is sent through different propagations paths. The Multiple Input Multiple Output (MIMO) technique uses multiple antennas in the transmitter and in the receiver to improve the performance of a wireless transmission [TV09].

2.3.3 Automatic Repeat reQuest Schemes

ARQ protocols are reliable data transfer protocols that are based in retransmissions. The receiver passes the information to the sender of what has been received with and without errors in order for the sender to retransmit what was not received correctly. The exchange of information between the receiver and the sender is performed by control messages [LCM84].

To allow error detection at the receiver, the sender must send additional bits (error detection code) beyond the original data. If an error is detected, the receiver discards the erroneously received data and requests a retransmission of the same data. This process is repeated over and over, until the data and the additional bits are successfully received.

2.3.4 Hybrid-ARQ Error Control Schemes

Hybrid-ARQ is a scheme where the FEC subsystem is combined into an ARQ system. When this combination is done in a proper way, the disadvantages of both schemes can be overcome. The FEC scheme allows the correction of frequent error patterns, decreasing the number of retransmissions and increasing the system throughput. Also, the combination of FEC and ARQ schemes gives the advantage when an uncommon error pattern is detected. In this case, the receiver requests a retransmission rather than passing the erroneous decoded code word to the end user [LCM84].

In resume, the Hybrid-ARQ has higher reliability and throughput than separate FEC and ARQ schemes respectively. With all these advantages, Hybrid-ARQ was chosen to be used in 3GPP LTE program [SBT11].

The Hybrid-ARQ schemes can be divided in two categories: Type-I Hybrid-ARQ and Type-II Hybrid-ARQ [LCM84], and will be approached on the following sub-sections.

2.3.4.1 Type-I Hybrid-ARQ

In type-I Hybrid-ARQ, a FEC coder is used at the sender and a FEC decoder is used at the receiver to detect errors in transmissions. The message and the error detecting parity bit are encoded using a FEC code in the sender. In the receiver side, the error correction parity bits are used to correct channel errors. The result of the FEC decoder is an estimation of the original message, plus the error detection parity bits, which is tested by the error detection decoder to determine if the message should be accepted or rejected.

This protocol can increase the system efficiency in certain scenarios, like for instance, when the message is long or when the channel signal strength is low. By adding extra FEC parity bits, the unsuccessful transmissions probability decreases. It is possible to have a coding gain if a compensation between the reduction of transmissions and the increase of message length is made.

In opposition, when the channel signal strength is high, the type-I protocol does not improve the efficiency, since the strong signal allows an error free message delivery and the FEC parity bits are wasted. So, in this case, it is more advisable to use plain ARQ protocols due to the difference of both protocols in matters of efficiency [CC84].

2.3.4.2 Type-II Hybrid-ARQ

Type-II Hybrid-ARQ was planned to operate with the efficiency of plain ARQ in good quality signal and obtain the improvement of type-I Hybrid-ARQ in poor quality signal.

In this protocol, the message is encoded and sent with error detection bits. The FEC parity bits are now sent in separate transmissions. When the first transmission is received error free, there is no need to send the FEC parity bits [CC84]. If in the first transmission the receiver detects an error, it saves the message and requests a retransmission. The sender retransmits the FEC error detection parity bits, which are then used by the receiver to correct the errors in the stored message.

So, the type-II Hybrid-ARQ protocol allows the system to adapt to changing channel conditions by implementing incremental redundancy [Wic95].

2.3.5 Multiple Input Multiple Output Scheme

Since the MIMO technique has become a standard for WiMax and 3GPP LTE [SBT11], it is important to give a brief description about the approach.

In MIMO scheme, the total transmission power can be divided among multiple spatial paths. This puts the capacity of the MIMO system closer to the linear regime to each spatial path, and therefore, increase the aggregated spectral efficiency.

To implement a MIMO communication system space-time codes are used with multiple transmitters to provide spatial as well as temporal redundancy in the data received by an array of antennas. Space-time codes can be used in two different ways: coding adjustments and fixed codes.

In the first way, the receiver informs the transmitter about the propagation channel information, so the transmitter can adjust its coding. This brings advantages in terms of capacity, but it can be difficult to apply in dynamic environments.

On the other way, fixed codes of various rates are used to share transmitted power equally among all spatial channels, offering good performance over all channels.

MIMO systems have advantages in relation to Single-Input Single-Output (SISO). MIMO presents less sensitivity to fading due to the existence of multiple spatial paths and needs less power.

2.4 Medium Access Control Protocols in Satellite Communications

A Medium Access Control (MAC) protocol defines rules for stations to access to the shared medium and for the communication with each other in an orderly and efficient manner [GL00]. Not all MAC protocols are suitable for satellite communications, due to the specific requirements, for instance, handling high propagation delay. A large range of protocols that are applied in Local Area Networks (LANs) and Wide Area Networks (WANs) cannot be used for this purpose [Pey99].

MAC protocols can be classified as distributed or centralized. The distributed MAC protocols are capable of listening the physical medium to detect any ongoing transmissions, also known as carrier sensing, and minimize the probability of occurring a collision using collision avoidance algorithms.

The centralized MAC protocols move all the arbitration and complexity to the BS. So, the BS decides which and when a MT can access the medium. This allows a higher throughputs and energy efficiency.

The centralized category is divided into Guaranteed, Hybrid and Random Access. The Hybrid access also is divided in Random Reservation Access and Demand Assignment [GL00]. In this thesis, it is important to give a more detailed explanation about the Random Access and Demand Assignment protocols, since they are used for the transmission and retransmission process, respectively.

2.4.1 Random Access Protocols

With Random Access protocols, each MT makes its own decision regarding when to access the channel. Since the protocols are contention-oriented and very susceptible to collision occurrences, there is no guarantee of a successful transmission.

The absence of control brings advantages to the random access because it is simple to implement and robust to varying demand. As a disadvantage of this type of protocols, the occurrence of collisions leads to a wasteful of the system capacity, which is relatively limited. Therefore, for bursty traffic, it is not appropriate to accommodate real-time ap-

plications or guarantee QoS [Pey99].

A list of protocols that use random access is presented in [Pey99]: Pure Aloha, Slotted Aloha and Selective-Reject Aloha.

In Pure Aloha, the ready stations transmit their packets in a non-synchronous way. When one or several packets collide, each station is aware of this occurrence and retransmits the packet after a random delay. This random delay has the purpose of providing stability to the protocol. Due to a high probability of packet collision, the Pure Aloha protocol presents a maximum throughput of 18%.

Slotted Aloha improves the original Aloha protocol, by imposing the synchronization of every packet transmission in a defined length of time slots. Thus, the number of packet collisions is reduced and the throughput can achieve up to a maximum of 37%.

In Pure Aloha, although the collision between packets is partial, the packet is totally destroyed. The Selective-Reject Aloha avoids the total destruction of the packet, by dividing the packet into sub-packets and giving to each one, their own header. Therefore, when a new collision occurs, only the sub-packets involved are retransmitted. In terms of efficiency, the Selective-Reject Aloha is better than the original Pure Aloha, but the insertion of the sub-packet headers limits the throughput to a maximum of 30% [Pey99].

2.4.2 Demand Assignment Protocols

Demand Assignment Multiple Access (DAMA) techniques permit a set of MTs to efficiently share satellite resources on a demand basis, using a FDMA or TDMA architectures to allocate capacity [Fel96]. A MT that receives a slot allocation in a particular frame may use it to send one or more frames. Depending on the fraction of capacity used for the signaling information, the efficiency may be above of 70%. The reservation on demand can be implicit or explicit [Pey99].

The implicit reservation is made through reservation of slots in subsequent frames. If a MT transmits a packet in a determined slot, that slot is associated to the correspondent MT and all the others are aware of this reservation. An example of this implicit reservation is the Reservation Aloha (R-Aloha) [Lar78]. Although the protocol can remove the set-up time to reserve a slot, there are disadvantages. It is not possible to prevent a MT

from successfully capturing all the slots in a frame for an indefinite time period [Ret80].

In explicit reservation, a single reservation slot is assigned to each MT in every frame. The reservation is made by a control subframe that consists of a sequence of bits and comes in each frame. This is also used to announce upcoming transmissions [Pey99].

Request-TDMA (R-TDMA)[CD01] is a good example of explicit reservation. The scheme uses a fixed-assignment technique for making reservations and allows the total, available channel capacity to be shared among all stations that are busy [Ret80].

2.5 Physical Layer Solutions

MAC protocols are traditionally used to solve collisions; however, they cannot handle all the possible cases. In [HKL97][ZR94] was observed that signal capture mechanisms can decode a packet that has a higher power, in comparison with all the other packets involved in a certain collision. This can be made by the Physical layer.

In the Physical layer, data is converted into symbols for transmission, and performed the reverse process for the reception. Also, it gathers the received data into frames which are passed to upper layers [BNNK08].

A Physical layer solution, to issues involving packet collisions is called MPR.

2.5.1 Multipacket Reception

MPR is defined as the ability of receiving and decoding more than one packet involved in collisions from concurrent transmitters [LSW12]. This characteristic allows a less restrained transmission of the packets in relation to the conventional MAC protocols, where only one packet is received at a given time [BCA12].

According to [LSW12], the MPR techniques in a wireless random network can be classified based on the Transmitter perspective, Trans-Receiver perspective and Receiver perspective, as shown in figure 2.3.

The Receiver perspective, in particular the Multi-User Detection (MUD), is the most relevant to the subject of this thesis, since it is present in the implemented receiver.

MUD techniques can be divided into optimal and sub-optimal. In the optimal techniques, the receiver is able to decode multiple users in parallel with great gains, but is

extremely complex to implement and computationally exhaustive [And05]. Therefore, the complexity associated with these techniques led to the investigation of low-complexity solutions as sub-optimal linear multi-user receivers [LV89].

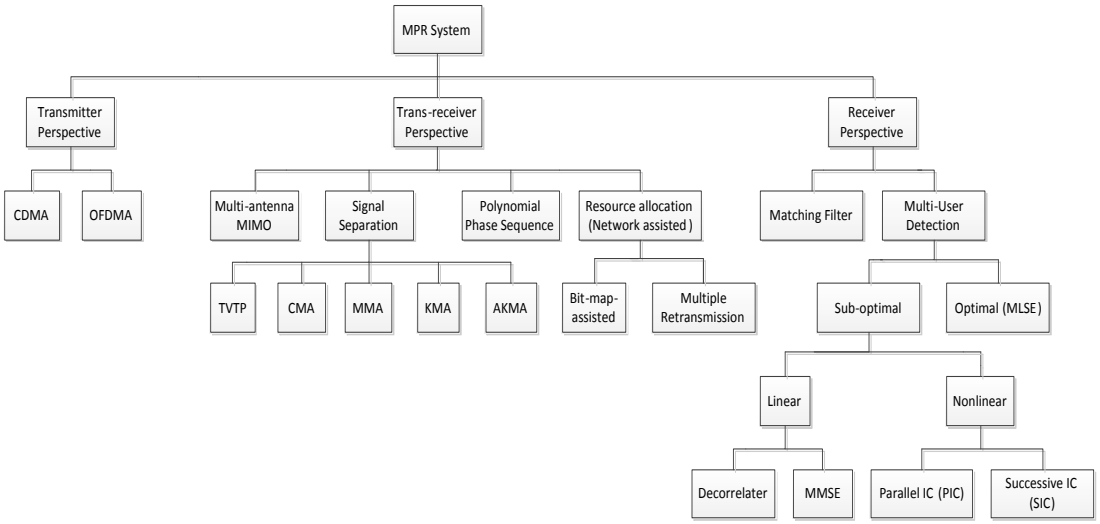

Figure 2.3: Classification of techniques applied for MPR [LSW12].

Sub-optimal MUD techniques are divided into linear and non-linear. The most known linear MUD techniques are the Decorrelated detectors and the Minimum Mean Square Error (MMSE) [LV90][XSR90]. They have the advantage of producing an optimal value for the near-far resistance performance metric. However, the high complexity is a disadvantage in comparison with the non-linear MUD techniques.

Non-linear MUD techniques use interference estimators and remove the interference from the received signal before the detection [LSW12]. The most known non-linear MUD is the Multi-stage Interference Cancellation (IC), which is divided in Successively Interference Cancellation (SIC) [WGLA09] and in Parallel Interference Cancellation (PIC) ways [BCW96]. Non-linear MUDs have a low complexity, but in terms of performance, the non-linear are worse than the linear MUDs.

2.5.2 PHY-MAC Cross-Layer

Cross-layer is the interaction between protocols from different layers of the Open Systems Interconnection (OSI) protocol stack, which share a common state. It is assumed that it is important to share information on lower layers in order to improve the performance

on higher layers in terms of wireless communications, despite the OSI reference model specifies that layers do not share information between them except through the interface.

This interaction gives advantages, since all layers are affected by wireless link characteristics, thus, the union among protocols at different layers allows adaptability to changing channel conditions [BNNK08].

There are several research works covering the design of to the cross-layer between the Physical and the MAC layers. In 2007, [GLASW07] published as study of a cross-layer MAC algorithm for Wireless Local Area Network (WLANs) considering an error free transmission, using single antenna terminals and multiple antenna access points. A year later, [HLZ08] unites the MPR protocol with MAC and proposes an adaptive resource allocation algorithm for MIMO WLAN. More recently, in [RP12] is studied a cross-layered PHY-MAC algorithm with MIMO and over a jittery channel, revealing a high Signal to Noise Ratio (SNR) and a low bit error rate.

Network-assisted Diversity Multiple Access (NDMA) research work is approached in the next sub-section, which is the base of this thesis project.

2.5.2.1 Network-assisted Diversity Multiple Access

NDMA [TZB00] is an approach to the collision resolution problem to recover packets from multiple collisions. Diversity combining and signal separation techniques are used in order to recover and retransmit the collided packets. In the NDMA scheme, in case of a collision between P users occur in a given time slot, the same P users repeat their transmission for a total of P times, so that P copies of the collided packets are received. The signal received from the collision is stored in memory, so that it can be combined with future retransmissions, allowing the extraction of collided packets information.

The protocol has the advantage of not imposing penalties to the throughput efficiency for multiplexing variable-bit-rate data sources, since the number of collided users is equal to the number of required slots.

Over the years some research work has been made to improve the NDMA protocol. The initial NDMA was designed for flat fading channels, which are not very appropriated for wireless communications. Because of this fact, in [ZT02] was created a new approach

for a frequency selective channel environment using multiuser receivers and CDMA systems. User Identification (ID) signature sequences were considered, with the purpose of making easier the collision detection and resolution process when multipath effects are present. Despite of achieving a good throughput performance with this technique, ID sequences also give disadvantages because they grow linearly instead of logarithmically with the number of users, introducing a considerable overhead process. Zhang et al [ZST99] present a method to resolve packet collision problem without the need of an orthogonal ID sequence. The method is called blind signal separation and is less computationally demanding in relation to the initial NDMA scheme, due to its proportionality to the number of colliding packets.

To improve the multiuser detection in NDMA protocols, it was presented a new resource allocation mechanism. This mechanism, developed in [SRGM07], adjusts the probability of false alarm of each user controlling the average number of active time-slots per user, which allows the regulation of the typical delay degradation of a fixed resource allocation scheme, ensuring different levels of QoS.

Madueno and Vidal [MV05] studied the usage of the NDMA protocol for broadcasting in ad-hoc networking with and without combining retransmissions. A new protocol was defined which does not require feedback from the receiver part.

2.5.2.2 Hybrid-ARQ NDMA

Hybrid-ARQ NDMA (H-NDMA) is the combination of an H-ARQ technique with NDMA, proposed in [GaPB$^+$11]. The H-NDMA access mechanism forces the MTs to transmit a quantity of packet copies greater than the number of collided MTs. The BS defines the time slots, which are used by MTs to send data frames. Several MTs could use a given channel, and the maximum number J that is doing it, is controlled by the BS. The BS has also the duty of detecting collisions and to inform the MTs that they occur through a broadcast downlink channel. After the involved MTs receive the collision information signal, they resend their packets.

In H-NDMA, the uplink slots are allocated in an organized way, in a sequence of epochs, and using an SC-FDE scheme for uplink proposes. The BS transmits a synchro-

nization signal (SYNC) to alert the MTs with new packets to transmit. Each epoch is defined by the number P of MTs that transmit data, and it was assumed that this number fits $1 \leq P \leq J$. When a collision occurs between P MTs, the base station requests P-1 retransmissions. Additional retransmissions are made if the error persists. Before each additional retransmission, an acknowledgment signal is sent by the BS to MTs, defining the ones that must retransmit at the next slot. The epoch ends when all packets are successfully received, or when the number of retransmissions is equal to the maximum allowed.

The H-NDMA presents advantages in terms of network capacity and packet delay, when compared with the classic NDMA and Hybrid-ARQ protocols. Increasead scalability was another characteristic shown by this new protocol.

2.5.2.3 Satellite NDMA

H-NDMA was proposed to enhance NDMA's error resilience capability, but is unsuitable for satellite networks due to the multiple control packets required to control additional retransmissions and acknowledgments. These introduce a delay and jitter incompatible with several kinds of QoS requirements [GaBD$^+$12].

The Satellite-NDMA (S-NDMA) protocol, proposed in [GaBD$^+$12], is very similar to the H-NDMA protocol by the fact that it also uses a combination of H-ARQ and NDMA protocols. The packet transmission process of the S-NDMA scheme can be seen in figure 2.4.

Individual packets are firstly scheduled to $P+n_0$ slots in an initial super-frame for P transmitting MTs, where $n_0 \geq 0$ defines a number of redundant retransmissions used to improve error resilience. In case of unsuccessful transmission, additional groups of slots may be scheduled in future super-frames, reducing the number of round trip times required to achieve a successful reception.

In comparison with the H-NDMA, the S-NDMA is more suitable for satellite networks, since it was especially designed to provide QoS guarantees for scenarios with a high RTT.

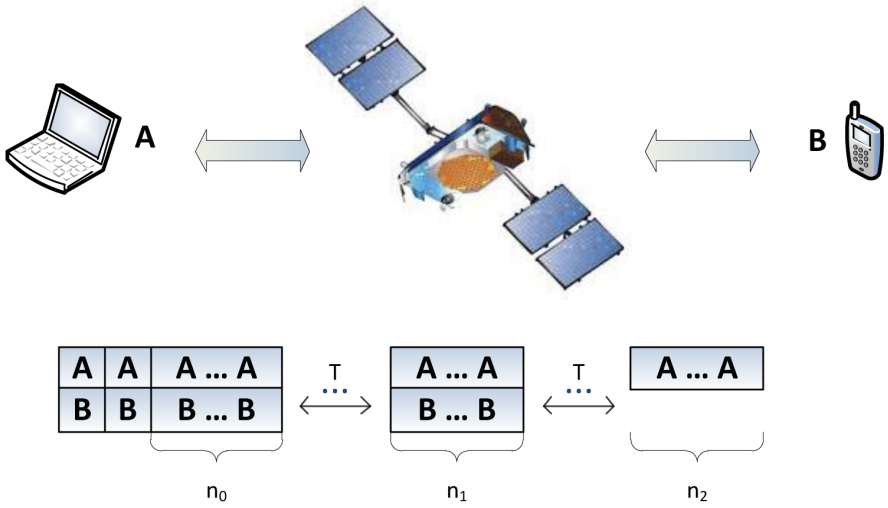

Figure 2.4: S-NDMA scheme signal [GaBD+12].

2.6 Quality of Service

When a connection is accepted into a network, certain conditions such as delay, delay variation (jitter), packet error rate (PER) or throughput, may be guaranteed by the system [AUB99]. This is called QoS, but the concrete definition is not entirely clear, since it does not exist a standard nomenclature.

In 2001, a general model for QoS is proposed in [Har01] with three levels: intrinsic, perceived and assessed [Har01].

Intrinsic QoS level considers all service features related to the Network Performance (NP), like network efficiency or resources. This guarantees the functions needed to the communication and is the key for quality perceived and accessed by the end-users.

The perceived QoS level is based in the experience of the customer on a specific service. It is influenced by the customer's requirements and opinions, as also what is offered and achieved by who is providing the service. Since customer expectations cannot be translated into a technical language, it is necessary to define in advance a Service Level Agreement (SLA), some parameters of quality and assessment criteria desired by the customer and corresponding to the ambitions of the service providers.

The assessed QoS level is related with the perceived QoS by the customer and their requirements, where the customer decides if he continues to use the service or not. The

facts of this decision are based in the perceived quality of the service, the associated costs and also the capacity of the service provider to resolve the customer complaints [SCJ11].

2.6.1 QoS Architectures for IP Networks

A main principle for the QoS architectures is to sustain end-to-end service models across a wide diversity of internet platforms. As an example of this architectures, the Internet Engineering Task Force (IETF) has conceived two architectures specifically to support guaranteed QoS for streaming multimedia.

First it created the Integrated Services architecture, where the main characteristic is to reserve bandwidth in advance to groups of users, supporting a multicast environment. It used the Resource Reservation Protocol (RSVP) based on a spanning trees supported by data structures in the router's memories, to route traffic for multiple senders to multiple receivers, also allowing singular receivers to transit between channels to eliminate congestion.

But there are some important downsides in the integrated service architecture like the reservation of resources to a large scale scenario and the vulnerability of the network to a possible loss of the per-flow state, that is internally stored in the routers. So IETF created another architecture called Differentiated Services based on the classification of the traffic. The treatment given to the packets is determined by the traffic class and the per hop behavior established. A packet can have a different requirement of delay or jitter associated to a specific service, like for instance, regular or premium, and so it can have a priority in the forwarding to another router [TW10].

2.6.2 Class of Service

The class of Service (CoS), also known as QoS class, relates the parameters of quality of service with types of traffic, network features and service applications. There are basically two main levels to describe the CoS: application and network.

The traffic classes are classified at the application level. There are four classification categories: non-elastic non-interactive (for video on demand or live television) and interactive (to voice over Internet Protocol, video teleconference and online gaming), elastic

non-interactive (like file download and sending e-mail) and interactive (web browsing and grid computing). The separation between non-elastic and elastic classification is based on the amount (fixed or dynamic) of bandwidth required by the application.

At the network level, there are several definitions for the most important classes, based on a set of applications and QoS parameters. It will be shortly described the definitions proposed by four organizations. The International Telecommunication Union-Telecommunication (ITU-T) proposed five service classes with different applications and a set of values for IP Packet Delay Variation (IPDV), IP Packet Error Ratio (IPER), IP Packet Loss Ratio (IPLR), and finally, IP packet Transfer Delay (IPTD), which are presented in table 2.1. These values are constraints for the traffic transported between the user network interfaces [SCJ11].

CoS	**Applications (examples)**	**IPTD**	**IPDV**	**IPLR**	**IPER**
Class 0	Real-time, jitter, high interaction	100 ms	50 ms	$1x10^{-3}$	$1x10^{-4}$
Class 1	Real-time, jitter, interactive	400 ms	50 ms	$1x10^{-3}$	$1x10^{-4}$
Class 2	Transaction data, highly interactive	100 ms	Undefined	$1x10^{-3}$	$1x10^{-4}$
Class 3	Transaction data, interactive	400 ms	Undefined	$1x10^{-3}$	$1x10^{-4}$
Class 4	Low loss only (video streaming)	1 s	Undefined	$1x10^{-3}$	$1x10^{-4}$

Table 2.1: ITU-T Classes of Service, examples of their application, and QoS parameters' values. [SCJ11].

2.6.2.1 QoS Traffic Classes

The Universal Mobile Telecommunication System (UMTS), managed by 3GPP, has established four QoS traffic classes. The Conversational class assures the time constraints required for real-time voice conversation and for video conferencing. This kind of traffic presents stringent transfer delay and transfer delay variation, a guaranteed bit rate and a restricted possibility of buffering (only with small size buffers). The Streaming class, unlike the previous class, allows buffering without buffer size restrictions, constrained transfer delay and transfer delay variation. It is used for audio/video streaming applications. The Interactive class does not have a limit to the transfer delay and the bit rate is

not guaranteed, but presents a low bit error rate. Web browsing and telnet applications are supported by this class. The Background class has the same characteristics of the Interactive, but does not request a response pattern for the destination at a given time, like for example, the email application.

Finally, IEEE has defined eight traffic types for the LAN networks in the 802.1d standard and four access categories in the wireless networks in the 802.11e standard. For the LAN network, each traffic type is differentiated by the user priorities. It only supports QoS requirements on the voice and video traffic, such as jitter and delay, supported by a priority mechanism. The services in the wireless network are classified as background, best effort, video and voice [SCJ11].

In the context of this thesis, it will be considered the Conversational class as defined by 3GPP , and the respective QoS constraints.

2.6.3 Real-Time Conversational Class

The Conversational class is designed to handle bi-directional real-time traffic between groups of human end-users. Examples that use real-time Conversational class are the voice over IP (VoIP) and video conferencing tools.

This class has the most demanding delay requirements in relation to the other three QoS classes. The Conversational class presents the strongest and most stringent QoS requirements.

For voice applications, the audio transfer delay requirements are directly linked to the interactivity of the end users. One-way end-to-end delay is advised to be limited to 150 ms and in the radio link the maximum delay should be less than 20 ms. Also it must be considered that the human ear is highly intolerant to short-term delay variation (jitter), and so it should be as low as 1 ms.

Video telephony implies full-duplex communication and requires that the audio and video appear synchronized, in order to match lip movements with the words being heard by the end user. The video telephony application is intend to have a maximum delay of 50 ms in the link radio and 400 ms end-to-end delay for images communication. Since the human eye is tolerant to some loss of information, it is acceptable a certain degree of

packet loss, depending on the video coder that is applied and the level of error protection used [AMCV06].

2.6.3.1 Audio Traffic

VoIP, IP-telephony or broadband telephony are terms that describe the same thing, namely transmission of the human voice over a data network, using the Internet Protocol.

As oppose to the ordinary PSTN, where every call has a dedicated connection between callers, in the VoIP calls the capacity is shared with themselves and with other kind of data as well [GL08].

VoIP presents several benefits such as, reduced communication cost, the usage of the integrated IP infrastructure and the participation in a multimedia application. Also, the advantages of packet-switched networks apply, like for instance, high network utilization while keeping the quality of circuit-switched networks. To minimize bandwidth consumption, VoIP carries voice data using speech data compression and/or header compression [DSM04].

The VoIP communication is basically made by three parts: data streams, call control and codecs.

Data Streams

VoIP usually sends data streams through Real-time Transportation Protocol/Used Datagram Protocol (RTP/UDP). RTP is an Internet standard protocol created to transport real-time data such as audio and video over an Internet. It consists in a data part which supports timing reconstruction, security, loss detection and content identification for real-time applications, and a control part that gives QoS feedback, identification and synchronization between different types of media streams [GL08].

UDP provides a way for applications to send encapsulated IP datagrams without establishing a connection [TW10]. Since the connection-oriented protocols introduce delay due to the retransmissions and congestion control, it is preferable to use UDP despite some data packet loss that can occur.

Call Control

Call control is made by a separate protocol such as H.323 standard by ITU-T, Session Initial Protocol (SIP) or Voice Activation Detection (VAD). VAD is used to monitor the RTP streams in a conversation while H.323 and SIP handle the initiation and termination of the session. A briefly explanation about the H.323 and SIP protocols is given in the annex A and in the annex B, respectively.

The VAD primary function is to provide an indication of speech presence in order to facilitate speech processing as well as possibly provide delimiters for the beginning and end of a speech segment. It is an important enabling technology for a variety of speech-based applications including speech recognition, speech encoding, and hands-free telephony [LB05]. The VAD algorithm begins by extracting some measured quantities from the input signal and compares it with thresholds values, given by the characteristics from the noise and speech signals. The values that exceed the thresholds are considered as voice-active [TO00].

VAD is able to increase the number of users and power consumption in portable equipment. Unfortunately, a VAD is far from efficient, especially when it is operating in adverse acoustic conditions, like for instance, when a conversation takes place in noisy environments [BCRS02].

Codecs

Codecs are used to compress and encode voice data for bandwidth optimization purposes. There are several levels of encoding with increasing benefits on voice quality and delay [GL08]. Two classes of voice streams can be generated by different codecs: constant bit rate (CBR) traffic streams and variable bit rate (VBR) traffic streams. VBR can be produced by codecs using silence compression and generating active (On) and inactive (Off) periods alternately. The second group is used in the VoIP application, namely the ITU-T Conjugate-Structure Algebraic (G.729 Annex B) coder [DSM04].

The G.729 B algorithm operates on 16-bit linear Pulse-Code Modulation signals at a bit rate of 8-kb/s. The speech signal is analyzed for speech frames of 10 ms corresponding to 80 samples, at a sampling rate of 8000 samples per second. The difference to the origi-

nal standard is that G.729 Annex B includes a silence compression method which allows using the VAD module [NGN+07]. Table 2.2 presents some examples of standard codecs, with the correspondent bit rate and coding delay.

Standard Codec	**Bit Rate (kbit/s)**	**Coding Delay (ms)**
G.711	64	0.125
G.726	16-40	2
G.729 A	8	15
G.729 B	8	10
G.723.1	5.3-6.4	30

Table 2.2: Standard codecs. [SCJ11].

Chapter 3

SR-NDMA Protocol Description and QoS

3.1 System Characterization

This thesis considers the uplink transmission between a group of MTs and a singular satellite from the LEO satellite system, working as a BS. MTs are low resource battery operated devices, capable of sending data packets and using SC-FDE to the uplink transmission. On the other side, a satellite is a high resource device that runs a multi-packet detection algorithm with H-ARQ error control in real-time. It also uses a receiver with MPR to resolve collisions and employs OFDM in the downlink transmission.

The SR-NDMA protocol establishes for the uplink channel, a continuous sequence of time slots, limited by the maximum bandwidth (B_{max} *slots*) per Round Trip Time (RTT). A set of time slots composes a super-frame. Slots can be Random Access (RA) or Schedule Access (SA). The number of RA and SA time slots defined in a super-frame are established by the satellite, which sends this information in a downlink control channel to the MTs. The MT's data packets are initially transmitted synchronously in the RA slots. The RA slots are allocated in groups of n_0 slots, each carrying a copy of the packet, in order to increase the total packet energy and redundancy available at the receiver. If the data packet is not successfully transmitted during the RA slots, it will be retransmitted in the SA slots of a new super-frame. The SA slots are also allocated in groups of n_l slots, for

the lth retransmission of a packet.

The sequence of super-frames in which a data packet is transmitted and retransmitted, is called an epoch. The maximum duration of an epoch is limited by the number of allowed retransmissions, R. In the end of the Rth retransmission, the data packets that could not be received are dumped from the queue.

3.1.1 Medium Access Control Protocol

A maximum number of MTs are accepted to form a group and share a set of time slots to send their data packets. The maximum number of MTs is defined by the MPR capability of the receiver. For the following sections, it will be considered a maximum of J MTs per group, and the same time duration for all data packets.

3.1.1.1 Random Access Mode

The satellite starts by allocating the RA slots, according to bandwidth and QoS requirements, for the initial transmission of the MAC data packets. The RA slots are grouped in sets of n_0 slots to each packet, carrying their n_0 redundant copies. The number of different packets transmitted in the RA mode is N, given a total of $N*n_0$ RA allocated slots per super-frame. Figure 3.1 represents an example of two packets sent by each MT, where in each slot is sent a copy of the correspondent packet.

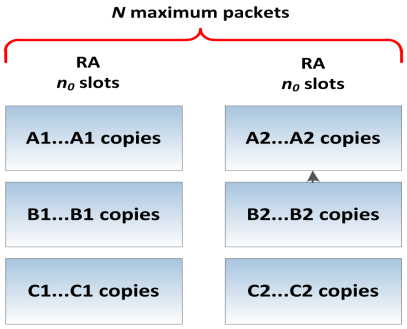

Figure 3.1: RA packet transmission.

Also is considered a period T equal to the highest RTT in a given MT set. The total usage of the N RA group slots depends on the number of packets in the MT's queue, so the number of MTs that transmit in each is RA slot is a random variable P, which satisfy $P \leq J$.

In order to maintain the energy and bandwidth efficiency, the n_0 value must be carefully planned. Also the maximum throughput of the system, limited by $(N * J)/T$, should be higher than the total load, λJ, where λ denotes the average packet generation rate per MT, to guarantee stability.

3.1.1.2 Scheduled Access Mode

After the initial transmission, the satellite gets to know that P MTs transmitted in the initial RA slots of an epoch. This allows the satellite to choose the values from n_0 to n_R, in which the data transmission is optimized.

In case of unsuccessful transmission in the initial RA slots, or generalizing, after the RA slots of the super-frame l, the SA mode schedules the necessary SA slots, limited to what is left of the B_{max} slots of the super-frame, to retransmit the data packets in the l+1 super-frame.

The number of retransmissions is limited by R, so the maximum length of an epoch is R plus the initial transmission. If the data packets are successfully received before the Rth retransmission, the epoch ends as well. After the Rth retransmission, the remaining data packets are dropped.

In the SA mode, the total number of slots allocated to a data packet in the lth super-frame of an epoch, is given by $\mathbf{n}^{(P)} = \left[n_0, {n_1}^{(P)}, ..., {n_R}^{(P)}\right]$.

Due to the high RTT value for a satellite network, and in the presence of delay requirements to guarantee QoS for the traffic class that is being used, the R value cannot be too high. So, R should be below $\lfloor \tau_{max}/T \rceil$, where τ_{max} is the maximum delay value, and $\lfloor argument \rceil$ represents the floor function, which returns the maximum integer below or equal to the function argument.

The throughput can also be limited by the availability of enough SA slots to transport all traffic. A super-frame has $B_{max} - (N * n_0)$ time slots to allocate SA slots.

3.1.2 Multipacket Reception Receiver Structure

In this thesis it is considered the use of the linear multipacket receiver running the MMSE detector for SC-FDE systems proposed in [GaDB+11]. An analytical expression for the

PER was obtained in [GaDB$^+$11] and is briefly described in this section.

Nodes contend for the channel at each epoch and as expected collisions might occur. A data block, of N symbols, transmitted by a user p, can be expressed, on the time domain, as $\{s_{n,p}; n = 0, ..., N-1\}$, and its correspondent on the frequency domain as $\{S_{k,p}; k = 0, ..., N-1\}$. At the receiver, at the frequency domain, the received signal from multiple MT's for a given transmission r is

$$Y_k^{(r)} = \sum_{p=1}^{P} S_{k,p} H_{k,p}^{(r)} + N_k^{(r)}, \tag{3.1}$$

where $H_{k,p}^{(r)}$ is the channel response for the pth MT at the rth transmission. $N_k^{(r)}$ is the channel noise for the rth transmission. The total number of slots allocated to an epoch until the $l+1$th super-frame for P MT's is given by $\zeta_l^{(P)} = \sum_{i=0}^{l} n_i^{(P)}$. Considering that P MTs transmit $\zeta_l^{(P)}$ times and $0 \leq l \leq R$, then the received $\zeta_l^{(P)}$ transmissions are characterized as follows

$$\begin{aligned} \mathbf{Y}_k &= \mathbf{H}_k^T \mathbf{S}_k + \mathbf{N}_k \\ &= \begin{bmatrix} H_{k,1}^{(1)} & \dots & H_{k,P}^{(1)} \\ \vdots & \ddots & \vdots \\ H_{k,1}^{(\zeta_l^{(P)})} & \dots & H_{k,P}^{(\zeta_l^{(P)})} \end{bmatrix} \begin{bmatrix} S_{k,1} \\ \vdots \\ S_{k,P} \end{bmatrix} + \begin{bmatrix} N_k^{(1)} \\ \vdots \\ N_k^{(\zeta_l^{(P)})} \end{bmatrix} \end{aligned} \tag{3.2}$$

For a given MT p, the estimated signal at the frequency domain is

$$\tilde{S}_{k,p} = \begin{bmatrix} F_{k,p}^{(1)} & ... & F_{k,p}^{(\zeta_l^{(P)})} \end{bmatrix} \mathbf{Y}_k = \mathbf{F}_{k,p}^T \mathbf{Y}_k \ . \tag{3.3}$$

$\mathbf{F}_{k,p}$ corresponds to the feedforward coefficients of the proposed system, and these are chosen to minimize the mean square error $2\sigma_{E_{k,p}}^2$ for a MT p. Considering that $\mathbf{\Gamma}_p = [\Gamma_{p,1} = 0, \dots, \Gamma_{p,p} = 1, \dots, \Gamma_{p,P} = 0]^T$, $2\sigma_{E_{k,p}}^2$ is evaluated as follows

$$\begin{aligned} 2\sigma_{E_{k,p}}^2 &= \mathbb{E}\left[|\tilde{S}_{k,p} - S_{k,p}|^2\right] \\ &= \left(\mathbf{F}_{k,p}^T \mathbf{H}_k^T - \mathbf{\Gamma}_p\right) \mathbb{E}\left[\mathbf{S}_k \mathbf{S}_k^H\right] \left(\mathbf{F}_{k,p}^T \mathbf{H}_k^T - \mathbf{\Gamma}_p\right)^H \\ &\quad + \mathbf{F}_{k,p}^T \mathbb{E}\left[\mathbf{N}_k \mathbf{N}_k^H\right] \mathbf{F}_{k,p}^* \ . \end{aligned} \tag{3.4}$$

Regarding $\mathbb{E}\left[|S_{k,p}|^2\right] = 2\sigma_S^2$ and $\mathbb{E}\left[\left|N_k^{(r)}\right|^2\right] = 2\sigma_N^2$, the optimal $\mathbf{F}_{k,p}$ is obtained by applying the method of Lagrange multipliers to (3.4), which results[1]

$$\mathbf{F}_{k,p} = \left(\mathbf{H}_k^H \mathbf{H}_k + \frac{2\sigma_N^2}{2\sigma_S^2}\mathbf{I}_{\zeta_l^{(P)}}\right)^{-1} \mathbf{H}_k^H \mathbf{\Gamma}_p \left(1 - \frac{1}{2N\sigma_S^2}\right) . \tag{3.5}$$

From (3.4) and (3.5) results

$$\sigma_p^2 = \frac{1}{N^2}\sum_{k=0}^{N-1} \mathbb{E}\left[\left|\tilde{S}_{k,p} - S_{k,p}\right|^2\right] . \tag{3.6}$$

The structure from the receiver is represented in figure 3.2.

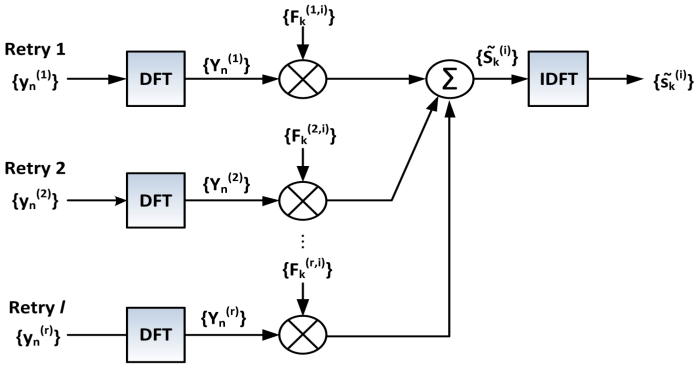

Figure 3.2: Receiver structure [PBD+13].

For a QPSK constellation and being $Q(x)$ the well known Gaussian error function, the Bit Error Rate (BER) of a given user p is

$$BER_p \simeq Q\left(\frac{1}{\sigma_p}\right). \tag{3.7}$$

For an uncoded system with independent and isolated errors, the PER for a fixed packet size of M bits is

$$PER_p \simeq 1 - (1 - BER_p)^M. \tag{3.8}$$

[1]It should be noted that σ_s^2 and σ_N^2 denote the variance of the real and imaginary parts of $S_{k,p}$ and $N_k^{(r)}$ respectively.

3.1.3 Analytical Average PER

Vieira et al [VGaB+13] considered an average PER for the packet transmission during the scheduled access phase. The behaviour associated to a packet transmission is defined by a hidden discrete-time Markov Chain, which is a sequence of events based on probabilities, where the current state of a system is independent of the previous states [LPW09]. The Markov Chain has a random state vector denoted by

$$\Psi^{(p,R)} = \{\psi_k^{(p,R)}, k = 0...R\}, \tag{3.9}$$

which defines the number of MTs whose packets were successfully received and stopped transmitting at the end of the retransmission super-frame $k = 0, ..., R$.

Considering only the retransmission super-frames up to $l \leq R$, the state space of $\Psi^{(p,l)}$ is denoted by the set $\Omega_p^{(l)}$. It contains all the vector elements $K^{(l)}$ (with dimension $l + 1$) that satisfy

$$\sum_{k=0}^{l} K_k^{(l)} = p. \tag{3.10}$$

Each state defines the set of transmission sequences where $K_0^{(l)}$ MTs stopped transmitting after the initial RA slots until $K_l^{(l)}$ MTs transmitted in the last l retransmission.

The average PER at the $(l + 1)$th super-frame with p MTs, $PER_p(\Psi^{(p,l)})$, and is also used to calculate the expected number of packets received with errors during an epoch until the lth retransmission super-frame,

$$\mathbb{E}\left[err\left(\Psi^{(p,l)} = K^{(l)}\right)\right] = K_l^{(l)} PER_p\left(\Psi^{(p,l)}\right). \tag{3.11}$$

So, the packet error probability for an epoch $\Omega_p^{(l)}$, considering that packet failures are independent, is

$$P_{err}\left(\Omega_p^{(l)}\right) = \sum_{K^{(l)} \in \Omega_p^{(l)}} \frac{1}{p} \times Pr\left\{\Psi^{(p,l)} = K^{(l)}\right\} \mathbb{E}\left[err\left(\Psi^{(p,l)} = K^{(l)}\right)\right]. \tag{3.12}$$

For more detail on the PER calculation, consult [VGaB+13].

Since the average PER is applied to a statical scenario, it cannot be used directly

in the simulator because each transmission depends on random factors. So, every time a transmission occurs, the PER value is calculated for that specific scenario using equation 3.8.

3.2 Traffic Generation

This thesis considers two different traffic generators that will be applied in the simulator. The first one is used to validate the analytical performance model of the SR-NDMA protocol. The second one models real-time traffic usually produced by a VoIP application.

3.2.1 Exponential Traffic Generation

Vieira et al [VGaB+13] assumed that each of the J MTs generates new packets according to an homogeneous Poisson process with rate λ, where the λ parameter is the average number of arrivals per unit time and each event is independent. The time between arrivals for a Poisson process can be determined using a exponential process, that is described as follows.

If the random variable X denotes the number of events which happen in a time unit, then

$$P(X = k) = \frac{\lambda^k}{k!} e^{-\lambda}. \tag{3.13}$$

Considering a Y random variable which is exponentially distributed with density function $\lambda e^{-\lambda x}$, so

$$P(Y \leq t) = \int_0^t \lambda e^{-\lambda x} dx = 1 - e^{-\lambda x}, \tag{3.14}$$

$$P(Y > t) = 1 - P(Y \leq t)) = e^{-\lambda x}. \tag{3.15}$$

The number of arrivals in a time interval T is defined by λT. So, the probability that exactly k events will occur in time interval T is

$$\frac{(\lambda T)^k}{k!} e^{-\lambda T}. \tag{3.16}$$

The event $Y > T$ means that the first arrival takes more than T units of time, which means that there are 0 arrivals in the first T units of time. Taking $k = 0$ in equation 3.15,

the result is

$$P(Y > T) = e^{-\lambda T}, \tag{3.17}$$

which makes the approximation between the Poisson and exponential distributions.

The total load injected into the system is controlled by a load factor (ρ) from 0 to 100%, given by

$$\rho = (\frac{\lambda J}{RTT}) * T. \tag{3.18}$$

Since the RTT value is equal to T interval, the λ value applied to random exponential generation for each MT is

$$\lambda = \frac{\rho}{J}. \tag{3.19}$$

3.2.2 Audio Traffic Generation

There are four main time periods to be considered for a typical real-time audio call modelling, which are represented in figure 3.3. The *inter-arrival* period gives the time between different call arrivals.

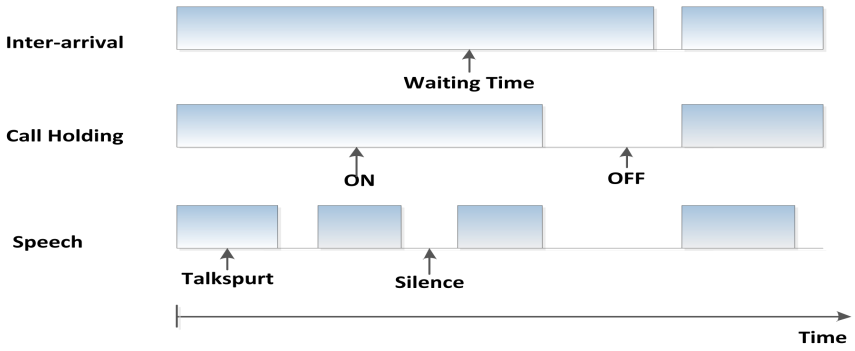

Figure 3.3: Real-time audio call model.

The *call duration*, which is the time that is reserved to hold a call, is defined by the *call holding* time with *ON* and *OFF* periods. In the *ON* period, the speech pattern is transmitted. It is composed with periods of *talkspurts* associated to continuous segments of speech and periods of *silence* with the absence of tone.

Dang et al [DSM04] proposed the use of a Generalized Pareto Distribution (GPD) for modeling the generation of *inter-arrival* time and *call holding* periods. The comulative

distribution function of the GPD is

$$F_{(\xi,\mu,\sigma)}(x)\ ) = \begin{cases} 1-(1+\frac{\xi(x-\mu)}{\sigma})^{-\frac{1}{\xi}} & for\ \xi \neq 0, \\ 1-exp(-\frac{x-\mu}{\sigma}) & for\ \xi = 0. \end{cases} \tag{3.20}$$

where ξ is *shape*, μ is *location* and σ is the *scale* parameter. The random GPD variable is given by

$$X = \mu + \frac{\sigma U^{-\xi} - 1}{\xi} \sim GPD(\mu, \sigma, \xi \neq 0) \tag{3.21}$$

or

$$X = \mu - \sigma ln(U) \sim GPD(\mu, \sigma, \xi \neq 0) \tag{3.22}$$

for a uniformly distributed variable $U \sim$ unif(0,1) [Hor13].

A model was proposed by [GL08] for the *silence* periods with GPD and the *talkspurts* periods with Log-normal distribution. The Log-normal distribution presents the following probability density function

$$f_x(x;\mu,\sigma) = \frac{1}{x\sigma\sqrt{2}\pi} e^{-\frac{(ln(x)-\mu)^2}{2\sigma^2}},\ x > 0 \tag{3.23}$$

where μ is the mean value and σ is the standard deviation. The random Log-normal variable is given by

$$X = e^{\mu+\sigma Z} \tag{3.24}$$

where Z is a normally distributed random variable with mean value 0 and variance 1 [CR12].

For the G.729 annex B codec modelling, the random GPD for both of *ON* and *OFF* periods is modelled in [DSM04].

[GL08] and [DSM04] provide statistical values for the time intervals considered for the audio application model presented in figure 3.1, and for the chosen codec. This values are reproduced in table 3.1.

	Main statistics		
Type	**Random Variable**	μ **[seconds]**	σ
Inter-arrival	GPD	21,18	448,43
Call holding	GPD	116,74	68789
Talkspurts	Log-normal	1,83	4,14
Silence	GPD	1,96	9,36
Codec ON	GPD	2,37	18,32
Codec OFF	GPD	1,56	5,19

Table 3.1: Main statistics values assumed for the VoIP call generation [GL08][DSM04].

These values defined considering for an audio sampling rate of 8 kHz and 50 packets sent in a second, which means that every packet carries 20 ms of audio, corresponding to 160 sample points. As referred in [VGaB$^+$13], for the LEO orbits considered, one RTT has a duration of 23.8 ms for the farthest MT. If a data packet is generated at every 20 ms during the *talkspurts* period, then the generation pattern corresponds to 26.9 time slots, which results in an average rate of 1.2 packets per RTT.

3.3 System Performance

The SR-NDMA simulator considers several performance features approached in the [VGaB$^+$13] analytical model. In this subsection, it will be demonstrated how that performance features were measured inside the proposed simulator.

3.3.1 Throughput

The throughput is calculated with the total amount of packets sent with success by the J MTs in the transmission or retransmission processes, during a determined RTT cycle interval (T_{RTT}) in slots. So, the throughput is measured by

$$S = \frac{\sum_{i=1}^{J} \sum_{k=T_{min}}^{T_{max}} x_{i,k}}{T_{RTT} * RTT} \tag{3.25}$$

where T_{min} and T_{max} are the minimum and maximum limit of T_{RTT}, and $x_{i,k}$ is the total amount of successful packets sent by a station i in RTT cycle k.

3.3.2 Packet Loss Ratio and Saturation Level

The throughput parameter can be used to calculate the packet loss ratio (ϵ) associated to packets that were dumped

$$\epsilon = 1 - \frac{S}{\rho J}, \tag{3.26}$$

and the saturation level (L_s) caused by total load injected into the system for a given N value

$$L_s = \frac{(\frac{S}{J}) * RTT}{N}. \tag{3.27}$$

3.3.3 Injected Load

Each MT injects the generated load in every RTT cycle ($\lambda_{i,k}$). The total load injected into the system is given by

$$L_T = \frac{\sum_{i=1}^{J} \sum_{k=T_{min}}^{T_{max}} \lambda_{i,k}}{T_{RTT} * RTT}. \tag{3.28}$$

3.3.4 Energy Per Useful Packet

Energy per useful packet ($EPUP$) is the medium energy used to transmit successfully a packet and it depends on the total number of packet copies ($C_{p_{i,k}}$) sent by the MT during a simulation

EPUP = (Energy spent/Number of packets sent) * (1/success rate) =

$$= \frac{(\sum_{i=1}^{J} \sum_{k=T_{min}}^{T_{max}} C_{p_{i,k}}) \times 10^{\frac{\frac{E_b}{N_0}}{10}}}{\sum_{i=1}^{J} \sum_{k=T_{min}}^{T_{max}} S_{p_{i,k}}} \times \frac{L_T}{\sum_{i=1}^{J} \sum_{k=T_{min}}^{T_{max}} S_{p_{i,k}}}, \tag{3.29}$$

where $S_{p_{i,k}}$ is the total amount of successful received packets in RTT cycle k by MT p_i. It is assumed that the data packets are retransmitted until they are successfully received.

3.3.5 Delay

The transmission packet delay of the SR-NDMA simulator is measured considering the number of slots between the packet generation and the successful reception, including the time in queue.

For a determined T_{RTT} interval, the delay is given by the average value of the subtraction between the transmission time and the generation time of every successful packet. The delay is also measured for the packets that were dumped by unsuccessful retransmissions. The intervals that contribute to the delay are represented in figure 3.4.

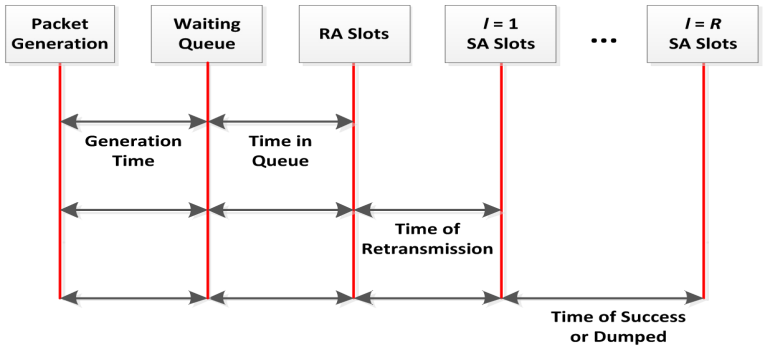

Figure 3.4: Possible time slots for delay.

3.3.6 Jitter

Considering that τ_T is the sum of every successful packet delay in a given T_{RTT} interval, the jitter can be measured by

$$\sigma_j \approx \sqrt{[(\tau_T)^2]_{avg} - [(\tau_T)_{avg}]^2}. \tag{3.30}$$

Chapter 4

SR-NDMA Simulator

This chapter presents a description of the SR-NDMA protocol simulator, emphasizing the used data structures, the interaction between modules, scheduling priorities, traffic generation and the application of a real-time traffic class.

The chapter is divided into two parts. The first part refers to the initial conception of the simulator to perform the operation of the MAC protocol. In the second part, a real-time traffic class is added to the simulator and its capability of satisfying QoS requirements is tested.

4.1 Simulator Implementation

The SR-NDMA simulator uses several modules to perform the MAC protocol, including the traffic generation. First it is presented the overall architecture of the simulator, followed by a detailed explanation of each module that composes the simulator.

4.1.1 General Simulator Model

The general scheme of the proposed Simulator will be presented in this subsection, as well as the interaction between the modules. The simulator illustrated in figure 4.1, is a black box, which receives a initial input configuration provided by the user and a file with values of n^P; returns a set of information logs; and internally performs an event sequencer (packet generation, packet transmission), which uses physical layer models to define what occurs in each step.

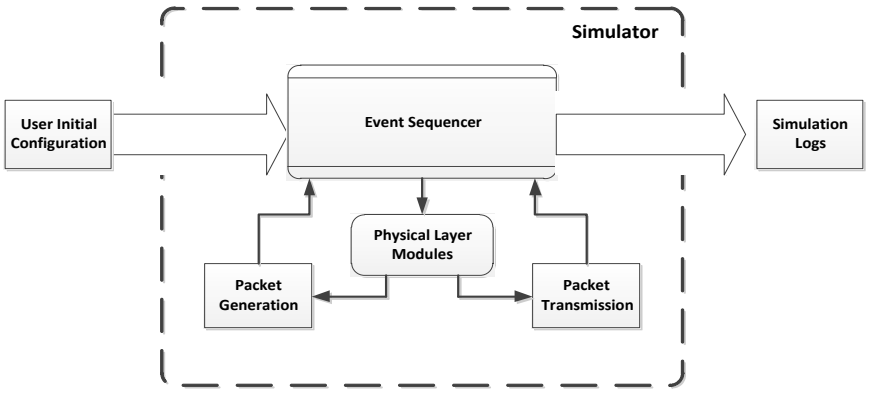

Figure 4.1: Simulator block diagram.

The simulator is composed by MT data structures; packet data structures; queue data structures; and information logs. The MT and packet data structures are used to keep current states of each entity. A queue data structure is used to store the several packet data structures. The transmission events related to the entire simulation are saved in the information logs, to be analysed later.

It has a main process, designated as *simulator*, which controls the advance of the simulation time (number of RTT cycles), and the access to the data structures in respect to the sequence of events. Each user has a waiting queue, which is managed by the simulator from a *packet generator* process, configurable for several types of packet generation. The *transmission* process manages the time slots (RA and SA) and models the behaviour of the physical channel.

4.1.1.1 Simulator System Dynamics

The user starts by defining a set of system variables, such as, the number of RTT cycles, the N packets that are sent in the RA slots, the number of MTs and the E_b/N_0 value at the satellite for each MT. It is also defined a file with the values of n^P, which specify the number of packet copies transmitted in each retransmission stage when P MTs transmit during the first transmission, for $1 \leq P \leq J$. Figure 4.2 presents the several functions made by the simulator.

In the beginning of a simulation the MTs are registered in the MT data structure. For each MT at each RTT, data packets are generated and injected into a waiting queue.

Figure 4.2: Simulator use case diagram.

At this point, the transmission process begins by removing packets from the head of the waiting queue and insert them in the RA slots. A random variable RND with an uniform distribution in the interval [0,1] is used to simulate reception errors: if RND is lower than the PER value for the scenario, the transmission fails and SA slots are allocated in the next RTT.

When a packet is removed from the system, the information inside the packet is saved in a log file, which is used by the statistical module. This module creates the output of the simulator, calculating the system performance metric. The execution flow of the processes presented in the simulator is shown in figure 4.3.

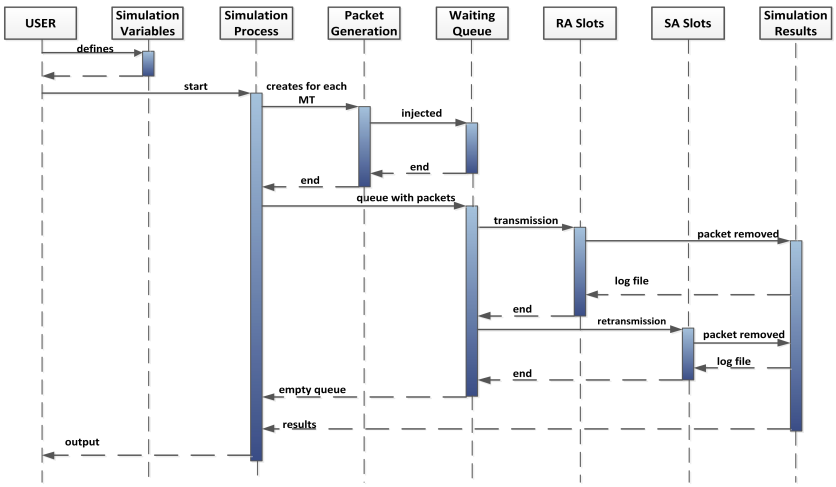

Figure 4.3: Simulator sequence diagram.

4.1.2 Initial Specifications

The SR-NDMA simulator is based on the main assumptions presented in the [VGaB$^+$13] research work. A LEO satellite constellation is modelled, with circular orbits at an altitude of 781 Km (like in Iridium), and a RTT of 23.8 ms for the farthest MT.

The severely time dispersive channel presented in [GaBD$^+$12] was considered, with rich multipath propagation and uncorrelated Rayleigh fading for each path and MT (similar results were obtained for other fading models). To cope with channel correlation for different retransmissions, the Shifted Packet technique from [DMB$^+$09] was considered, where each transmitted block has a different cyclic shift. MTs transmit uncoded data blocks with $N_s = 256$ symbols selected from a QPSK constellation with Gray mapping with an 814,9 μs transmission time, which is spread with a factor of 128. Therefore the RTT is defined as $T = 32$ slots, making $B_{max} = 32$ slots.

The Simulator also provides the possibility to configure other system parameters such as: the maximum R retransmissions, the E_b/N_0 value, the maximum number of J MTs and the the size of Q_{max}. Also it is possible to create several groups (G) of J MTs for scenarios with more than $T = 32$ time slots. For this thesis, and based in the [VGaB$^+$13] specifications, is considered a constrain of $PER_{max} \leq 1\%$ for $R = 2$, E_b/N_0 between -4 and 12 dB's and a MT set composed by $J = 5$ MTs, which corresponds to a smoothed conversational class with relax delay constraints. Contrarily to [VGaB+13], the Q_{max} is not bounded.

4.1.3 Data Structures

The simulator considers an uplink transmission of a group of MTs to a satellite. Data packets from the MTs are placed in a queue, waiting for an available time slot for transmission. There are three main entities in this process: MT, packet and queue.

The MT data structure contains information about:

- **Identity** - For each MT is assigned a number for identification purposes.
- **Group** - The group number to which the MT was entered (not applicable for the current T scenario).

- **Sequence number** - Registers the number of the last packet generated.
- **Last time** - Registers the time of the last packet generated.
- **Inter-Arrival** - Receives the *inter-arrival* period of the present call.
- **On Hold** - Receives the *on hold* period of the present call.
- **Speech** - If the current state is *talkspurt* or *silence*.
- **Speech Duration** - The duration of the current speech period.
- **Next Time Arrival** - The *inter-arrival* period of the next call.
- **Next Time Hold** - *on hold* period of the next call.
- **Current Time** - Keeps track of the current time slot.

Some of this fields are not use for exponential load, namely: the *inter-arrival*, *on hold*, *speech*, *speech duration*, *next time arrival*, *next time hold* and *current time*.

For each MT, a MT data structure is created, which is then combined into an array of structures of the type MT. The array is updated during the entire simulation, with the information of the last packet sequence number and the time of generation for each MT.

When a MT injects data packets to the system, it is necessary to save important aspects related with time, packet copies and the retransmission process. The packet structure adopted has the following fields:

- **Info MT** - Receives the identification of the respective MT.
- **Packet Number** - The packet's sequence number.
- **Generation Time** - The time when the packet is created.
- **Number Retransmissions** - Counter retransmission number.
- **Success Probability** - Is generated a random success probability to the packet to be compared with the result of Equation 3.8.
- **PER** - A matrix with every PER_p generated for each transmission.

- **Total Slots** - Number of copies transmitted during the last super-frame.
- **Number Copies Used** - The amount of copies that were sent.
- **Time In Queue** - The time when the packet enters in the waiting queue.
- **Time Out Queue** - When the packet is removed from the waiting queue.
- **Time Release** - When the packet is successfully transmitted or when is dropped.

Two packet queue types were created to store the data packets. When the new packets are injected into the system, they are stored in the waiting queue, and they are only released when a RA time slot is available. The second queue type stores the packets of unsuccessful transmissions or retransmissions, which can be sent in future SA time slots. Figure 4.4 represents an example of the interaction between data structures in the simulator.

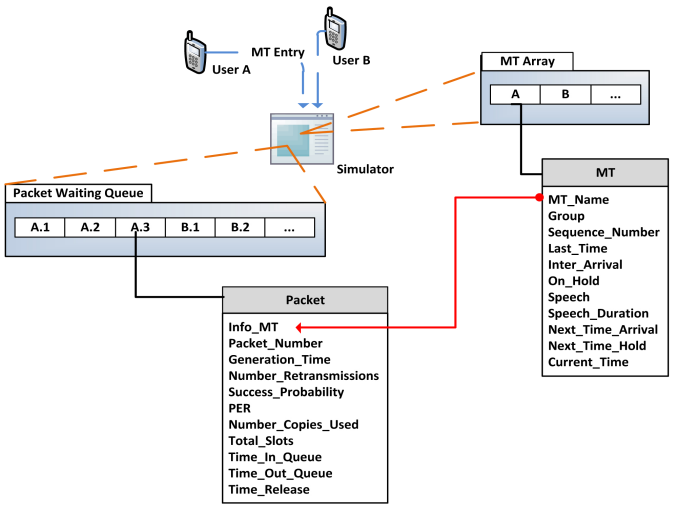

Figure 4.4: Interaction between data structures.

In this case, two MTs structures are registered in the MT array. When a packet is generated, it receives the identity of the respective MT and it is inserted in the Packet Waiting Queue.

4.1.4 Random Traffic Generation

The data packet generation is implemented defining a generator function for the inter-packet times, which may cross several RTTs.

Figure 4.5 represents the data packet generation process. The simulation starts with the calculation of an initial interval $\boldsymbol{Ts_0}$, before the creation of the first data packet.

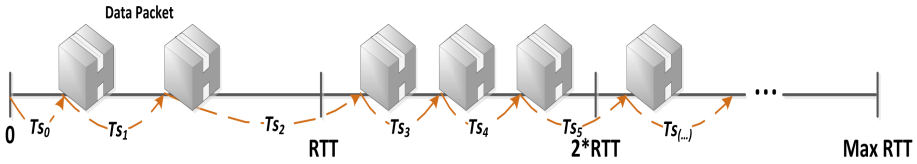

Figure 4.5: Packet generation sequence.

Subsequently, it is calculated a random number considering the distribution of the inter-packet time of a given source. If the next packet arrival time slot is still in the current super-frame duration, the process continues until it passes the end of the super-frame, which happens with $\boldsymbol{Ts_2}$, for the example of figure 4.5. The last time value is stored in the MT structure, to be used in the next random generation process. The total generation process ends when the maximum duration that was stipulated to the simulation is reached.

The first traffic generation object implemented was a Poisson traffic generator. This generation is made based on a random exponential variable with a mean parameter of $1/\lambda$, where λ is the load of a MT. Since the generation of any packet is an independent event, a random exponential variable gives the time between arrivals.

4.1.5 Time Slots and Packet Copies Combination

The simulation time is determined with the number of RTT cycles set by the user. The RTT time slots for transmission and retransmission of redundant packet copies, can also be initially configurable.

The distribution of RA and SA slots in a super-frame is influenced by the $\boldsymbol{n}^P$ matrix. Vieira et al [VGaB+13] showed that for a Poisson load there exists a $n^{P\star}$ matrix that minimizes the EPUP for a given load, a level of E_b/N_0 and for a determined number of P MTs. The first element of that matrix (n_0) defines the number of RA slots used by each packet for a given RTT.

The total number of RA slots in a super-frame is defined by Nn_0, being the first slots allocated in the simulator as RA. The total number of SA slots available for the retransmission process, is given by $N_{max} - Nn_0$. The concrete usage of the SA slots, is

defined by the (n_l) value for the respective l retransmission and depend on the number of packets that are retransmitted.

4.1.6 Packet Error Rate Calculation

The PER for a giving scenario is calculated using a module which simulates the SC-FDE with Iterative Block Decision-Feedback Equalizer (IB-DFE) uplink receiver. This module receives as parameters the E_b/N_0, a H_k matrix with the channel response to P MTs transmitting concurrently and a x_i matrix representing the slots where the MTs transmitted until the current super-frame during the transmission epoch.

An example of a possible x_i matrix is shown in figure 4.6, where 5 MTs transmit considering $R = 2$ and a combination of $n^P = [5, 2, 1]$ copies (i.e. 5 copies to be used in the RA slots, 2 copies for the first retransmission in the SA slots, and 1 copy for the last retransmission in the SA slots). Each MT transmit concurrently 5 copies of their correspondent data packets in the RA slots. A unique RND value is generated and compared to the PER, leading to independent failure possibilities for the MTs transmitting. In the next super-frame, for the other four (2,3,4 and 5) MTs, 2 SA slots are scheduled to allocate more copies for the retransmission process. The process continues until it reaches the last retransmission allowed, or until all packets are successfully received.

The PER module calculates a value for each MT that transmits a packet in the current super-frame. Each time a packet is transmitted, the PER function is called to calculate a new PER value with the specifications of that retransmission, using the Equation 3.8.

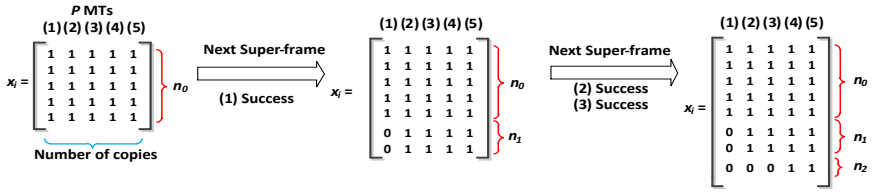

Figure 4.6: *x_i matrix for P=5 MTs.*

4.1.7 Scheduling Priorities

Data packets can be sent in RA slots or SA slots. New packets are firstly transmitted in RA slots. No packet differentiation is assumed in the system, so the next packet to

transmit in the RA slot is always in the head of the waiting queue. So, the packets that were introduced in the previous RTT can be transmitted immediately if the waiting queue has no more packets waiting for transmission.

For SA slots, it is established a priority in terms of the number of performed retransmissions. First the packets that have the highest number of retransmissions are searched in the unsuccessful transmission queue. If some SA slots are available, the search is made for second highest number of retransmissions, and so on, until all pending packets are retransmitted or no SA slots are available. This allows a reduction in the delay for the packets with more retransmissions.

The diagram in figure 4.7 represents the packet allocation process in the SA slots, where l denotes the number of times that the packet was retransmitted. This value is decremented until it reaches zero, which causes the process to be completed.

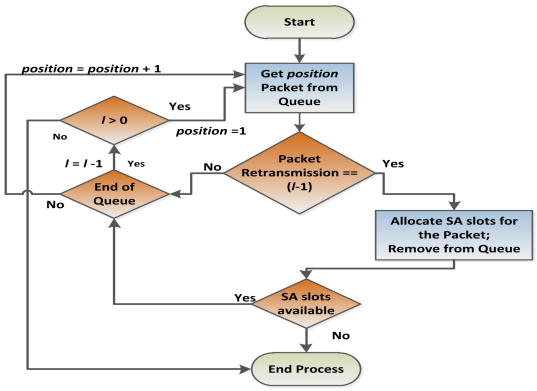

Figure 4.7: Packet retransmission process.

4.1.8 Packet Removal and Stored Information

A data packet is removed from the simulator queues when it is transmitted or when it is dropped due to successive unsuccessful retransmissions. The simulator has an information log which is filled in the moment of removal, with all fields of the data packet structure. The information log also keeps track of the data packets that are injected into the system. When the simulation process is terminated, the information log is used to calculate the performance metrics of the system, including, throughput, energy consumption, delay, and jitter.

4.2 Real-Time Audio Modeling

A new audio traffic generator was created, which that is composed by two modules to generate random data packets and to simulate the codec ON/OFF periods. The audio generation uses the full MT data structure, since it is necessary to guarantee that the MT saves the last interval when the call state has commuted to a new one and to maintain the information between RTTs.

4.2.1 Audio Random Traffic Generation

As was explained in subsection 3.2.2, the VoIP traffic generation considers periods of time for call settings and for speech pattern. Packets are only generated in *talkspurts* periods, since the codec suppresses the silence packets and sends a signal for the user to recognize that the call is still running. Figure 4.8 represents the entire process of random packet generation developed for the simulator.

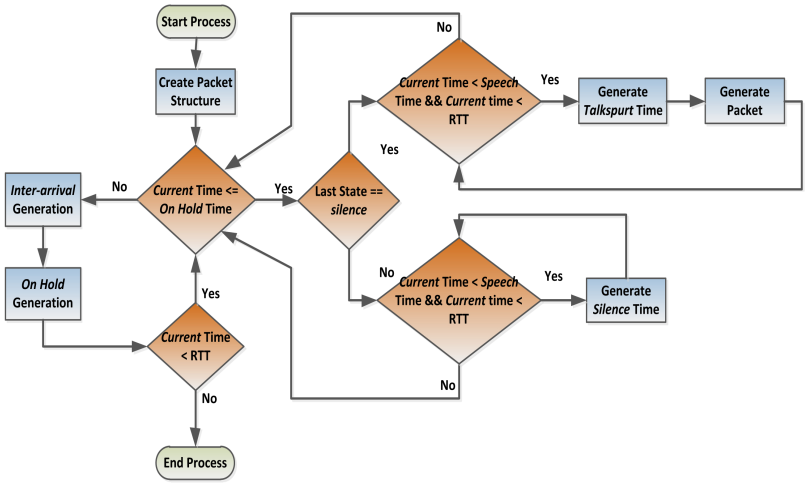

Figure 4.8: VoIP packet generation process.

The process begins by creating the packet data structures to allocate the information of the new generated packets. If a call already exists, the *inter-arrival* time and the *on hold* time are consulted from the MT structure to compare with the current time; otherwise new times are generated for the next period. It is also verified the last state of the speech pattern, to decide the new state.

If the previous state was *silence*, the new generated period will be a *talkspurts*, and

for the duration of that period or while it is not achieved the RTT limit, data packets are generated with a rate of 27 time slots per RTT.

4.2.2 Codec Implementation

The codec has two modes of operation: *ON* and *OFF*. In the *ON* mode, the data packets from the *talkspurt* speech of a conversation are injected into the waiting queue. Data packets generated during the *OFF* period are not queued.

The generation process transit between ON mode and OFF mode alternately. First is generated an *ON* period that is followed by an *OFF* period. The process is repeated until the time reaches the limit of RTT cycles considered for that simulation. The generated interval values are stored in a two line array for each state, which is the output from the codec module. This matrix delimits the *ON* and *OFF* periods. An example of a possible codec matrix is shown in figure 4.9.

The first *ON* interval consists in the initial slot and the generated time of the random GPD distribution with the parameters established for the *ON* state. Then, the generated value is used to be the first value of the *OFF* interval with the respective random *OFF* generation.

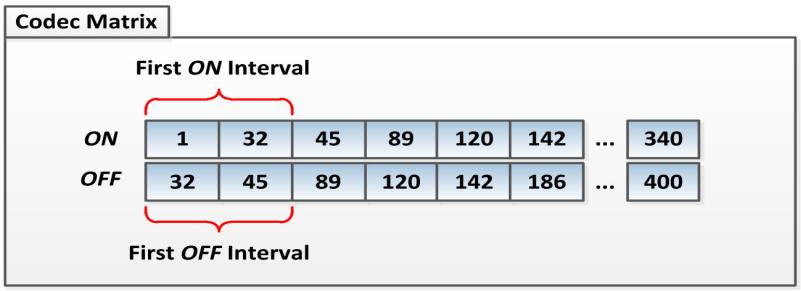

Figure 4.9: Codec *ON/OFF* matrix.

4.2.3 Integration of Audio Modules

Given the average data rate of 1.2 packets / super-frame of the audio generator presented in the subsection 3.2.2, the N value is defined as $N = 2$.

Relatively to the previous simulations presented in 4.1.1, for the audio simulations is selected the audio codec module instead of the Poisson generator. The codec is integrated in the beginning of the simulation process, thus creating the codec matrix to be used in

the simulation. For scenarios that support audio and data traffic generation, both codecs can coexist in the same simulation.

The values presented in the table 3.1 of the 3.2.2 subsection are converted into time slots to be applied in the random GPD and Log-normal functions.

When data packets are injected into the waiting queue, they are verified according to the *ON* mode. An iterative search is made between the states and to the end of the matrix to find the adequate interval for the data packet time. The new simulator sequence diagram is represented in figure 4.10.

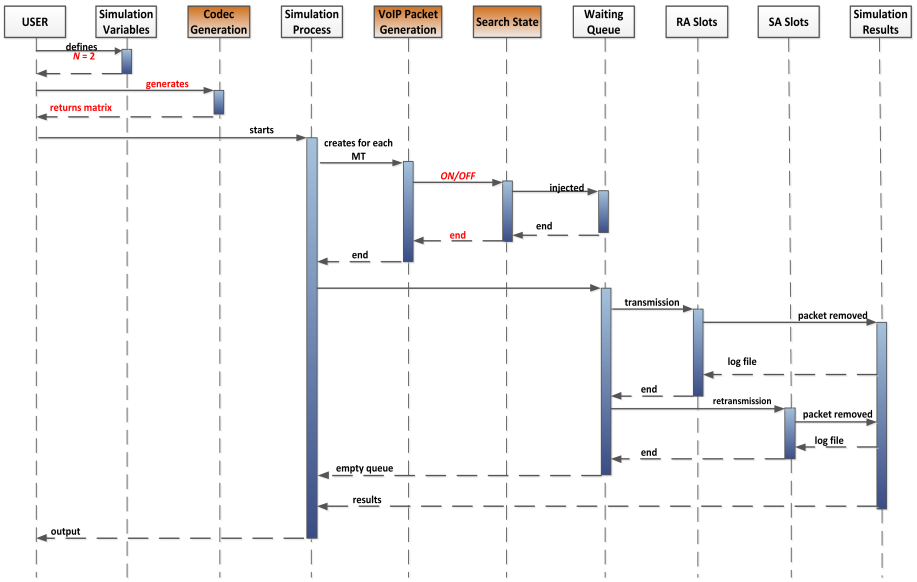

Figure 4.10: Final sequence diagram.

Chapter 5

Performance Analysis

In chapter 4, it was presented the simulator structure and the modulation of a real-time traffic class implementation. A set of simulations tests were executed in the MATLAB® environment to compare the protocol performance for simulated results and the analytical model. The capacity to fulfil the QoS requirements of a real-time traffic class was also tested.

This chapter is composed by into two parts: the validation of the simulator implemented and the study of its performance with audio real-time traffic.

5.1 Validation of the SR-NDMA Simulation Model

The main objective of this section is to validate the simulator reproducing a set of test scenarios that can be modelled by the analytical performance model in [VGaB$^+$13]. Notice however that while [VGaB$^+$13] considers a finite queue, the simulator considers a unbounded queue. The set of simulations were made using fixed values of $E_b/N_0 = 0$ dB and 12 dB, $n_0 = 7$ (for 0 dB) and $n_0 = 3$ (for 12 dB) redundant copies and a duration of 1000 RTT cycles. It is defined the $n^{P\star}$ matrix with the values that satisfy the QoS requirements and minimize the energy consumption, calculated in [VGaB+13] and reproduced in Annex C.3 for the correspondent P and E_b/N_0 values. The mean PER values of the analytical model of the Annex C.3 are also used to define the PERs for the correspondent transmission/retransmission scenario.

In the tests, we varied the number of packets sent in the first transmission by $N =$

$[1, 2, 4, 8]$ and the load factor by $\rho = [0.05, 0.1, 0.15, ..., 0.95, 1]$. The results of these simulations are shown and analysed in the next subsections.

5.1.1 Load and Saturation Level

The first verification made to the simulator is if the load injected into the system by a MT is well regulated by the ρ. The ρ is directly applied into the random exponential traffic generation as showed in equation 3.19. Since the maximum number of J is 5, the maximum load permitted per MT is obtained considering the total load saturation limits ($\lambda J = 1$), which is 0.2 packets/slot for J=5. Figure 5.1 illustrates the total load of a MT being controlled by several values of ρ.

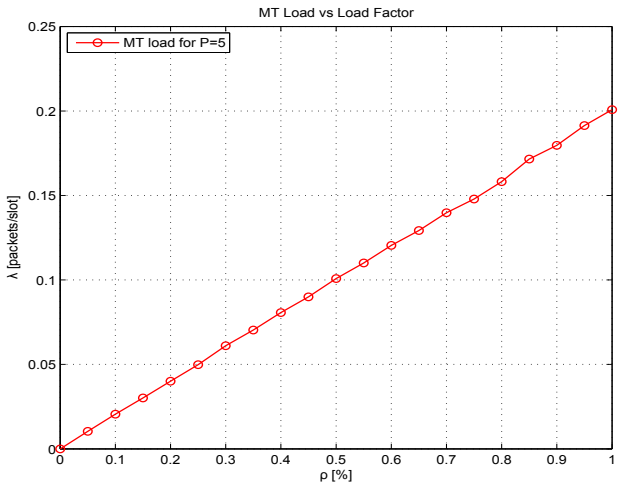

Figure 5.1: The MT total amount of load for a determined ρ.

The L_s, presented in equation 3.27, provides the information about the percentage of RA slots that is being used by the system. Figure 5.2 depicts the saturation level, where it is clear that this level is directly related to N, which defines the number of new packets that can be sent per RTT. With a lower N, the system saturation is achieved earlier than with $N = 4$ or $N = 8$. This is shown in figure 5.2, where the saturation begins with 15% for $N = 1$ and with 30% for $N = 2$. The best performance is achieved with $N = 8$, where the L_s is 80% for the full capacity.

It is also possible to verify the effects produced for a low energy level. For a higher N value, considering 0 dB, the amount of SA slots available is reduced. This produces

a bottleneck effect for lower E_b/N_0 values (0 dB), caused by the increased number of retransmissions in SA slots. On the contrary, higher E_b/N_0 values (12 dB) use less SA slots, and are more capable of handling high loads.

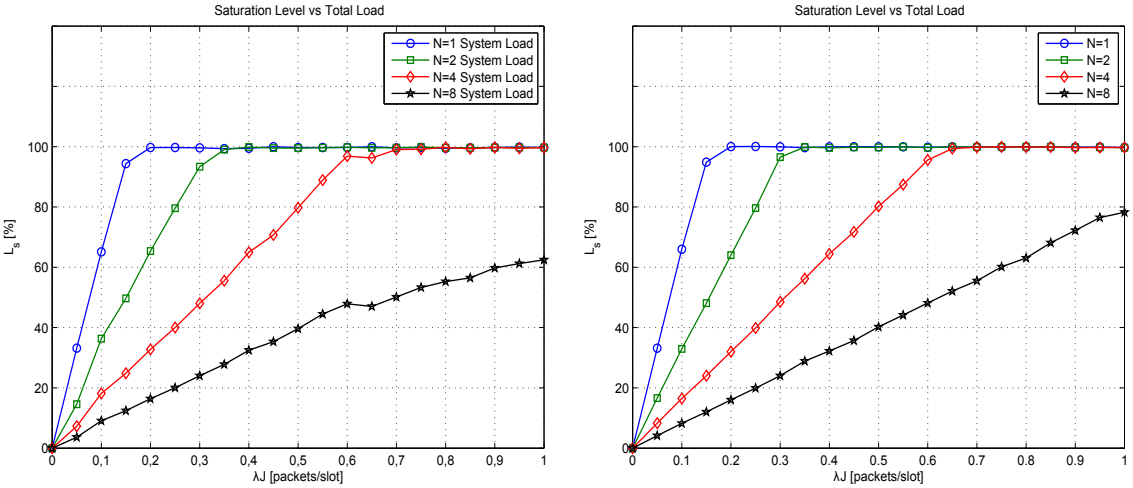

Figure 5.2: L_s for: 5.2(a) 0 dB; 5.2(b) 12 dB.

5.1.2 Throughput and Packet Loss Ratio

Figure 5.3 presents the average rate of successful packet delivered into the system for several levels of total load, calculated using the theoretical analytical model and the simulation results.

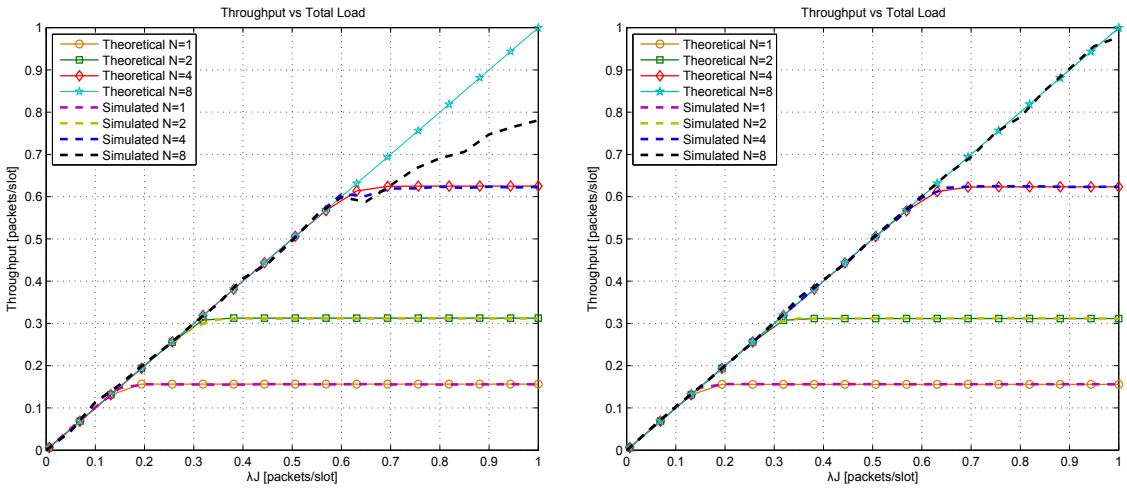

Figure 5.3: System throughput for: 5.3(a) 0 dB; 5.3(b) 12 dB.

For the 12 dB scenario, the throughput curves of both approaches are much similar for all the N values considered, which show that the simulator is properly modelling the bandwidth and correctly sending data from all MTs.

The throughput for each N is linked with the saturation level, since it becomes constant when the systems saturates (L_s reaches 1). It only does not reach saturation for $N = 8$ with $E_b/N_0 = 12$ dB.

In relation to the 0 dB scenario, the described bottleneck effect of the subsection 5.1.1, is verified for the $N = 8$ simulation curve. For the maximum load value, the difference of both curves is approximately 20%.

Figure 5.4 illustrates the packet loss ratio behaviour of both approaches. The packet loss ratio is calculated using the throughput, as described in subsection 3.3.2. Again, the curves of the theoretical protocol and the simulator are much similar. Naturally, the packet loss ratio is higher for low N values, because the system can not handle the amount of load that is injected by the MTs. The best performance is achieved with $N = 8$ and $E_b/N_0 = 12$ dB, where almost every packet in the waiting queue is transmitted.

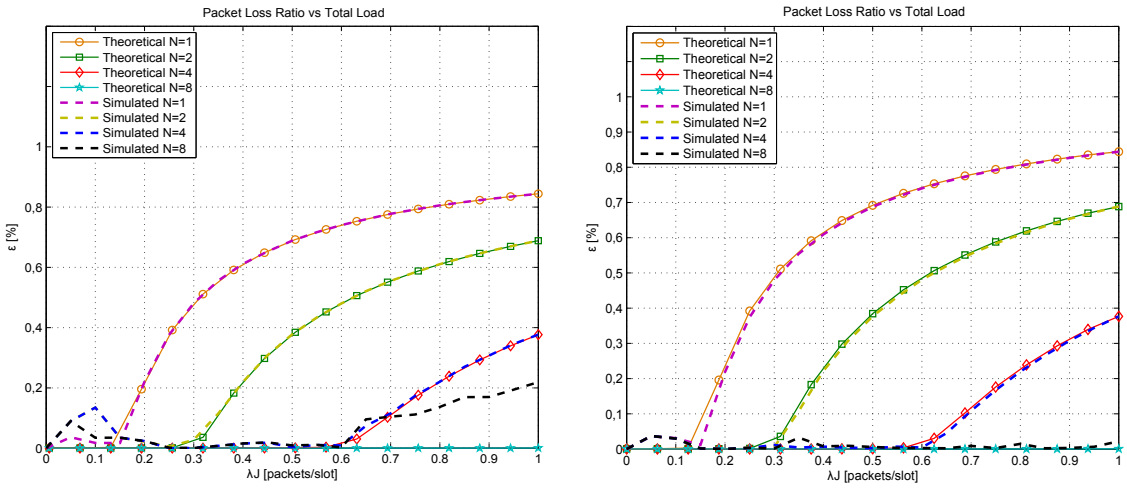

Figure 5.4: Packet loss rate for: 5.4(a) 0 dB; 5.4(b) 12 dB.

5.1.3 Delay and Jitter

The transmission packet delay is severely affected by lower N values, since the number of packets transmitted can not keep up with the amount of load that is injected into the

system, which causes the congestion of the waiting queue. This is also represented by the saturation level, that gives the information about when the system is going to choke.

Figure 5.5 illustrates the mean average delay of both approaches, until it is reached the saturation point.

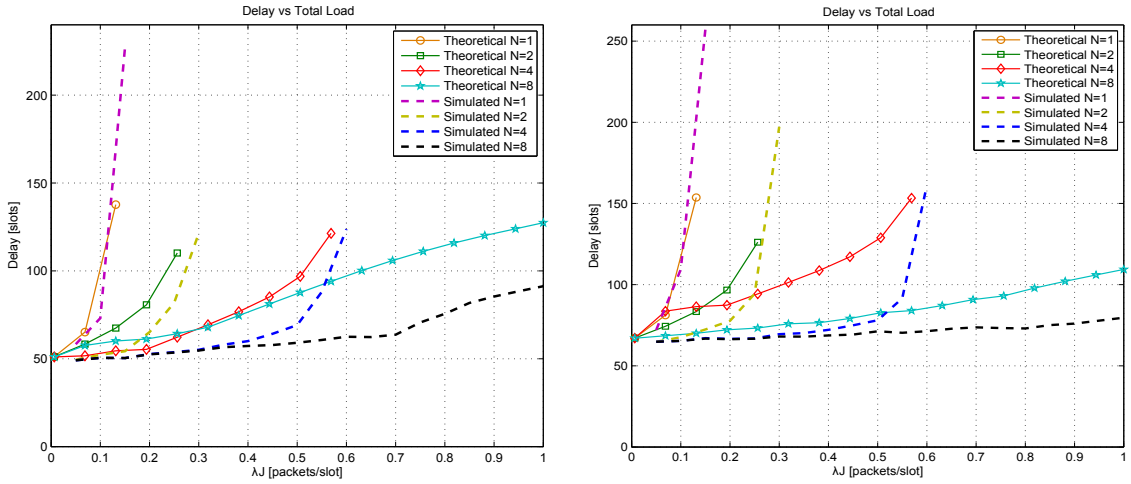

Figure 5.5: Mean transmission packet delay comparison for: 5.5(a) 0 dB; 5.5(b) 12 dB.

The difference in the queue sizes also introduce a most relevant difference: the analytical model defines a queue size of 25 packets, which imposes a delay limit for the system. In contrast to that, the simulator has no limit for the waiting queue, and that is the reason why figure 5.5 only shows the delay behaviour until the maximum throughput is achieved - above that value, it tends to infinity. The analytical model also does not accounts the queueing delay while waiting for a free SA slot, which is responsible for the higher deviation between the analytical and simulation delay values for 0 dB compared to 12 dB.

The system jitter is approximated by the standard deviation of the packet transmission delay in this dissertation, which is depicted in figure 5.6. $E_b/N_0 = 0$ dB scenario.

It can be seen that the analytical model provides a good approximation for the measured simulation values. The jitter is influenced by the same factors as delay: it decreases for higher N values. For the maximum total load and with $E_b/N_0 = 12$, the lowest jitter is achieved for $N = 8$ with a value of approximately 40 slots or 29.8 ms.

The bottleneck causes a severe effect in the $N = 8$ curve, for the $E_b/N_0 = 0$ dB scenario.

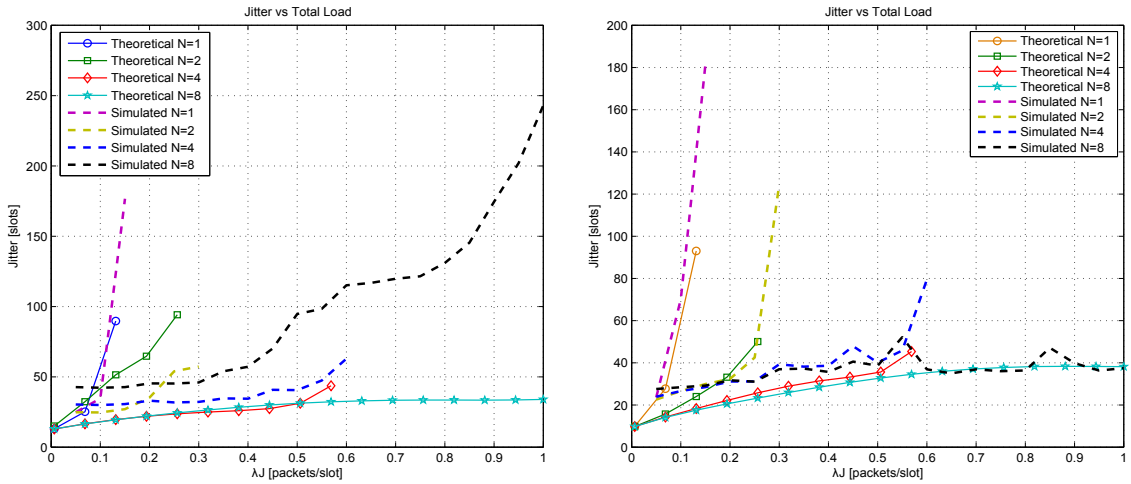

Figure 5.6: Jitter comparison for: 5.6(a) 0 dB; 5.6(b) 12 dB.

5.1.4 System EPUP

The energy consumptions for the simulated scenarios of 0 dB and 12 dB is presented in figure 5.8. The following results are based only in the assumption made in subsection 3.3.4. It is clear that EPUP is significantly lower for $E_b/N_0 = 0$ dB, although it supports lower loads.

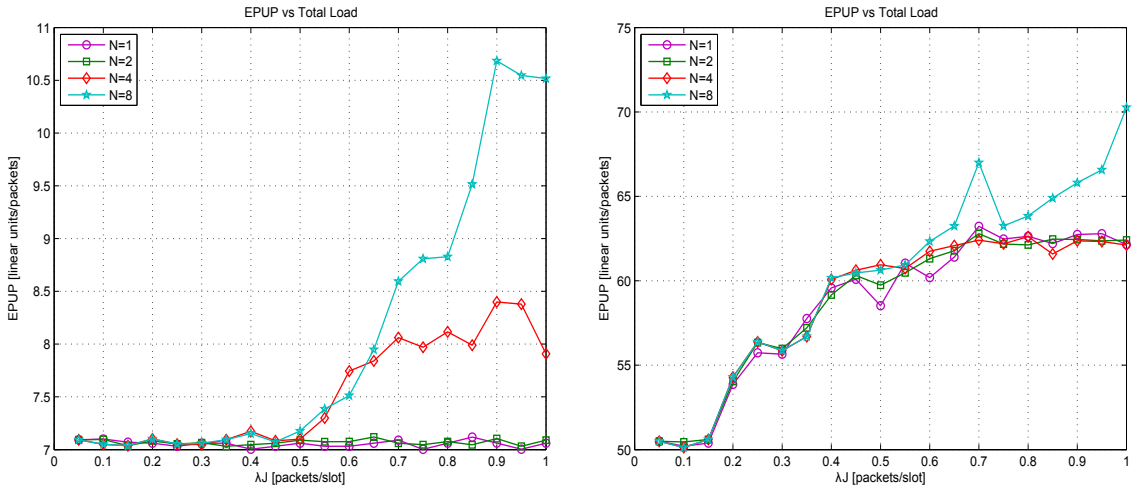

Figure 5.7: EPUP comparison for: 5.7(a) 0 dB; 5.7(b) 12 dB.

5.2 SR-NDMA with Audio Traffic Simulation Performance

For the audio simulations a fixed $N = 2$ was considered because the audio generation pattern is fixed. As described in subsection 3.2.2, the generation pattern is 1.2 packets (26.9 time slots for each packet) per RTT. To support this, the $N = 2$ value is adequate for $T = 32$ slots. In order to look for the system configuration that optimizes energy efficiency, n^P was varied, and the following settings were tested: $E_b/N_0 = [-4, -3, -2, ..., 11, 12]$ dB. In order to find the optimal n_0 we started from the optimal values for Poisson traffic, and verified if they also apply for this traffic class, by performing the simulations with several n^P matrices with small variations of the values around the Poisson optimal values, i.e. [$n_0^\star$ - 1, $n_0^\star$, $n_0^\star$ + 1] copies. Although it is added/subtracted a packet copy to $n_0^\star$, the total number of packet copies established by the analytical model was respected, and also $n_0 \geq n_1 \geq n_2$. So it is removed/added a copy to n_1 or to n_2, according to referred requirements.

Due to the random nature of the *talkspurts/silence*, *inter-arrival/on hold* and codec *ON/OFF* periods, the load rate varies in time, producing a set of performance results that may be influenced by the duration of the test, if it is too short. The audio simulations were performed with T_{RTT}=[500, 1000] RTT time slots, to verify if the chosen duration for the simulation interferes with the results.

5.2.1 Statistical Analysis

A simulation is composed by several iterations related to the given user settings. It is performed a simulation for each E_b/N_0 value, considering the possible [$n_0^\star$ - 1, $n_0^\star$, $n_0^\star$ + 1] values.

For the following measurements analysis, it is considered the T_{RTT} duration (this can be parametrized) to acquire the information provided in the log files. It is performed a separation between received packets and dumped packets, for counting purposes. Then is calculated from each packet: the duration between the packet generation time and the moment when it is received (with success) or when it is dumped and the total number of copies for the successful received packets. At last, the equations presented in subsection

3.3 are used with the retrieved data to produce the performance metrics.

5.2.2 Throughput and energy efficiency

Since the total amount of load of each simulation has a random nature, the throughput analysis is made in relation to the respective total load. Figure 5.8 illustrates the success rate ($S/\lambda J$) for each level of E_b/N_0, using the considered packet combinations. It is possible to see that the addition or the subtraction of one to $n_0^\star$ (with the subsequent adjustments for $n_1^\star$ and $n_2^\star$), affects the relation of the total injected load and the throughput for lower E_b/N_0 values. An higher $n_0^\star$ allows an higher throughput.

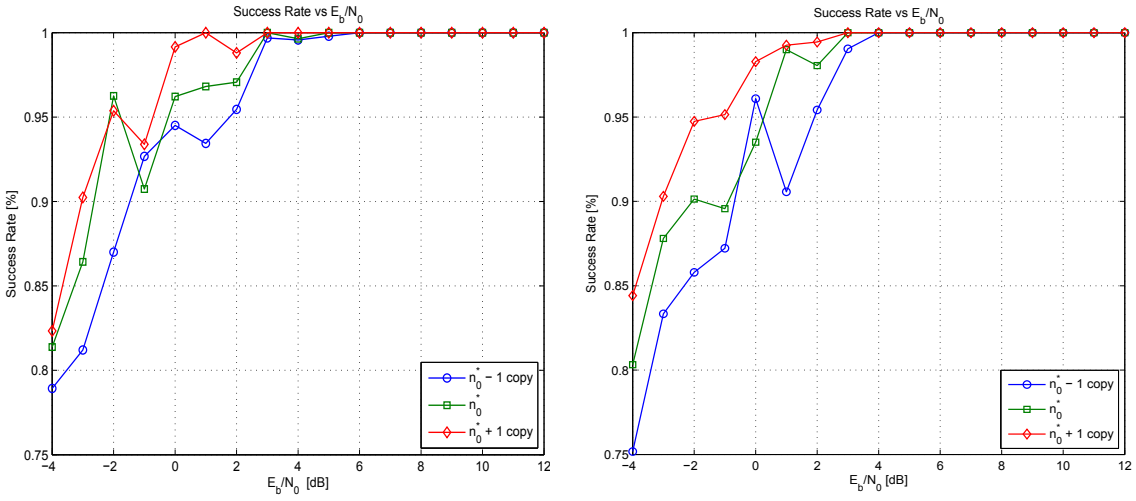

Figure 5.8: Success Rate for: 5.8(a) 500 RTT cycles; 5.8(b) 1000 RTT cycles.

With $E_b/N_0 \geq 3$ dB, the full transmission success is almost achieved for all configurations.

It is also possible to verify exists several fluctuations and irregularities exist in the variation of the curves with E_b/N_0. This can be explained by the non-linear variation of $n^{P^\star}$ configuration with E_b/N_0 (less copies are sent when the energy is increased) with a specific energy, which may produce a higher or lower PER level in comparison for the previously configuration.

Figure 5.9 depicts the system's EPUP for several E_b/N_0 values in relation to the $n_0^\star$. For lower levels of energy, the three curves are almost overlapped. When it reaches the maximum success rate, the addition of a packet copy is relevant in some results, the difference for the $n_0^\star$ can be about 10 dB/packet.

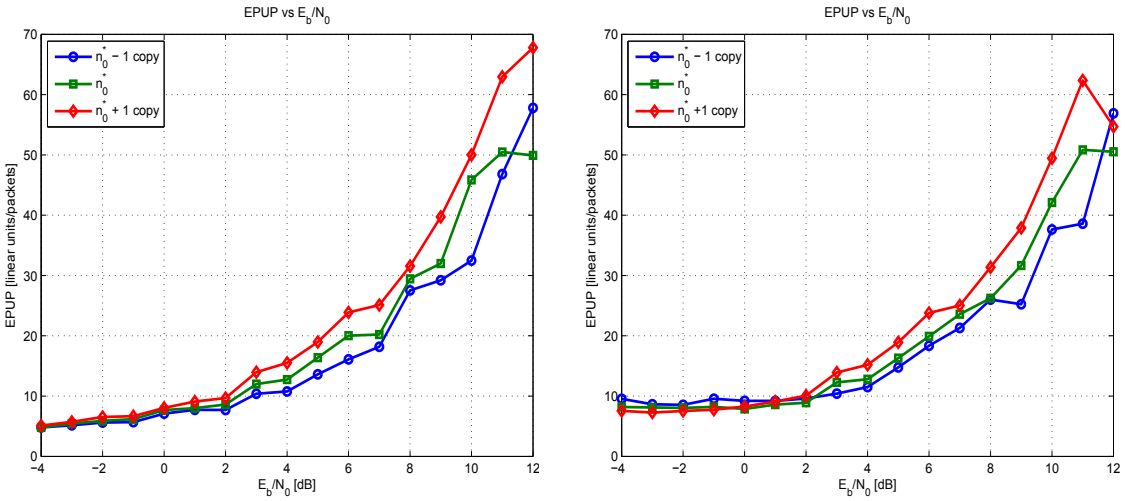

Figure 5.9: EPUP results for: 5.9(a) 500 RTT cycles; 5.9(b) 1000 RTT cycles.

5.2.3 Mean Delay and Jitter

For the SR-NDMA simulator, the QoS analysis was focused in the mean delay and jitter measurements of the system, which should be compared to the limit values defined in subsection 2.6.3, for the audio real-time QoS.

The maximum delay specified for the system is 150 ms (approximately 200 time slots). In figure 5.10, for both maximum RTT cycles, the three n_0 curves are below this limit.

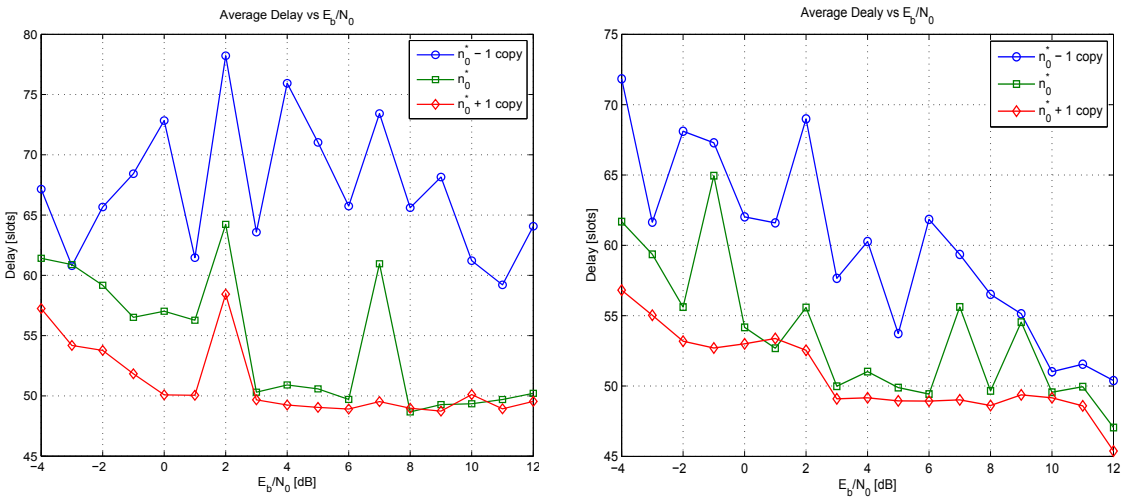

Figure 5.10: Average Delay results for: 5.10(a) 500 RTT cycles; 5.10(b) 1000 RTT cycles.

This guarantees that the chosen N value was appropriate to handle the audio pattern

generation, because the system does not enter into saturation.

Similar to what has been observed for the success rate variations, the total load injected into the system and the configuration shifting also causes fluctuations in the mean packet delay. This is more flagrant when a packet copy is subtracted, since the probability of requiring an additional retransmission increases, leading to an higher delay and jitter.

Figure 5.11 shows the jitter performance associated to the packet delay. The maximum advised value for the jitter is 1 ms (approximately 2 time slots). It is possible to see that even with the additional packet copy, the jitter requirement was not fulfilled. This is caused by the fact that most packets are sent in different stages (transmission and possible retransmissions), and not in a single one. Its effects can be alliviated by introducing a dejittering buffer at the receiver, which compensates the measured jitter.

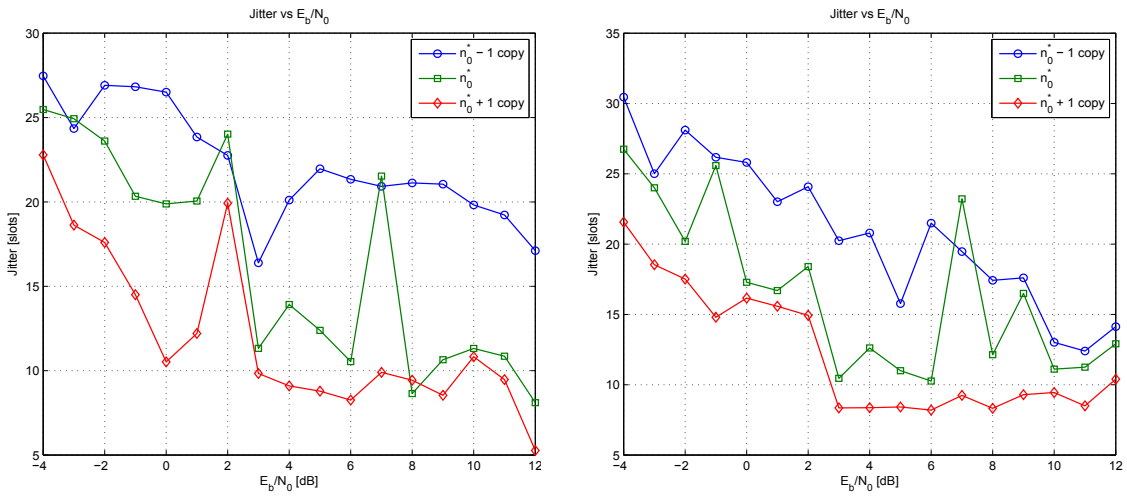

Figure 5.11: Jitter results for: 5.11(a) 500 RTT cycles; 5.11(b) 1000 RTT cycles.

This is an important factor, since it can deteriorate the conversation, with packets arriving in advance or later, regarding the correct data packet sequence.

5.2.4 Simulation PER Comparison

Figure 5.12 shows the comparison between the average global PERs of the audio simulation and the Poisson load used in the validation of the simulator. It is shown the average PERs of the three transmission stages defined for this thesis: the initial transmission using RA slots; the first retransmission; and the second retransmission. The simulation PERs are

obtained from each PER generated to a data packet during the epoch duration.

Although both PERs are from different traffic simulations, they present a similar behaviour for each simulation stage for various E_b/N_0. For the last retransmission, the probability of success in the reception of a packet is almost assured.

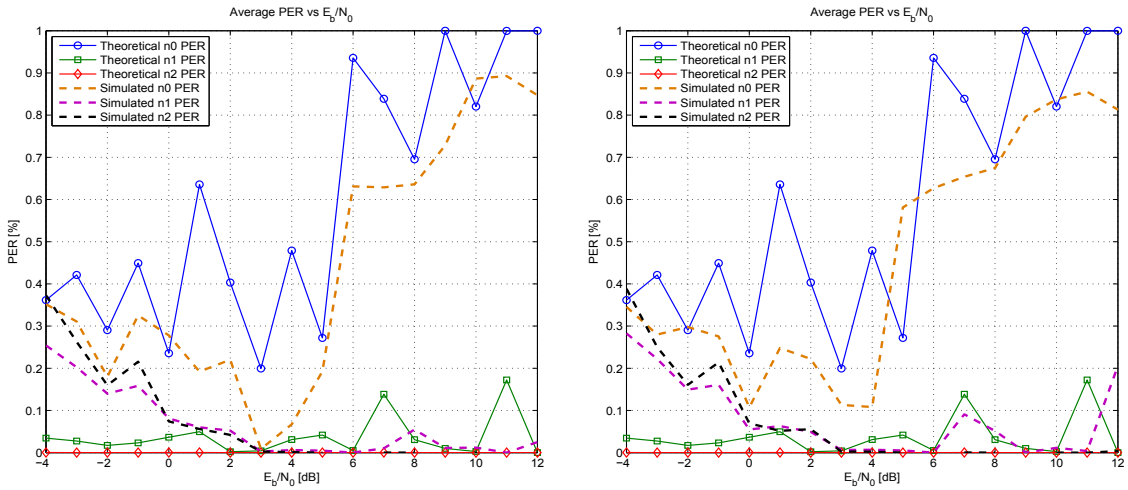

Figure 5.12: Comparison of the theoretical and simulated average PER results for: 5.12(a) 500 RTT cycles; 5.12(b) 1000 RTT cycles.

5.3 Overall Analysis

In the validation section, the results obtained by the simulator are very close to the results of the SR-NDMA protocol. The throughput and packet loss rate curves are almost perfectly overlapped with the protocol curves. For the delay and jitter simulation, the results have a similar behaviour to the protocol, although with some discrepancies that was caused by the non-definition of a limit to the waiting queue. In general, the simulator obeys to the requirements and the specifications of the protocol, assuming for that, the optimal combination of packet copies and E_b/N_0 values for a given number of MTs and load.

The inclusion of the audio real-time traffic class brought some challenges to the system configuration. In order to cope with the varying load, the value of N, which controls the number of packet that are taken from the waiting queue at every new transmission, should be properly defined to support the average load, but also the occasional bursts that may

appear It can also be seen that the two different T_{RTT} values did not influenced the simulations outcome.

With the results from the EPUP, mean delay and jitter, it is possible to verify that the $n^{P^\star}$ copies balances the energy consumption for higher levels of E_b/N_0, with the delay and jitter curves.

In general, the SR-NDMA simulator audio performance guarantees a high rate of success in relation to the packet reception, within the advised maximum limit for the delay, although, the jitter requirement was not achieved. Is also important to note that the huge delay value in a satellite network makes almost impossible to achieve the jitter goal, except when all packets are received after a unique transmission. However, this leads to an higher EPUP.

Chapter 6

Conclusions

This thesis analyses the performance of the SR-NDMA protocol, including its capability of providing QoS guarantees for real-time multimedia traffic, on satellite networks.

A simulator was implemented using the MATLAB® environment. A detailed explanation about the simulator modelling was presented in section 4.1. Several simulation tests were performed with a Poisson generation process traffic to validate the existing analytical model. The similarity between the analytical model and the simulation results for the two chosen energy levels proved their correctness. Also, it is shown that the optimizations performed for the SR-NDMA protocol can actually balance the throughput, delay, jitter and energy consumption.

A real-time traffic generation module was developed to analyse the SR-NDMA performance in response the real-time QoS requirements.

Simulation tests were performed by varying the optimal packet combination copies, referred by the SR-NDMA protocol. In section 5.2 is presented several measurements and a comparison between delay/jitter results and the respective QoS limits. Only the jitter requirements was not achieved, due to the very long propagation time, which would force the transmission of all packet copies in a single burst.

6.1 Future Work

The implemented SR-NDMA simulator presents a good launching base for other applications. This is assured by the parametrization of several system features. It is also possible

to add different modules to the simulator. The coexistence of more than one type of module is also assured.

As future work, it would be interest to analyse scenarios with RTT $>$ 32 slots (for example 64) and with several groups of MTs. This is already possible with the current simulator.

The addition of a graphical interface would turn the simulator more user-friendly, with several combinations of traffic generation and codecs to choose.

Appendix

Appendix A

H.323

H.323 is as an architectural solution for Internet telephony. Several protocols are specified for speech coding, call setup, signalling, data transport, and other areas. In Figure A.1, it is possible to see the general model. On the left side there is a zone composed by a gatekeeper that controls the endpoints in a LAN network. The H.323 protocols are applied in the Internet area, where several communications devices called terminals are connected. In the middle is a gateway that connects the Internet to the telephone network.

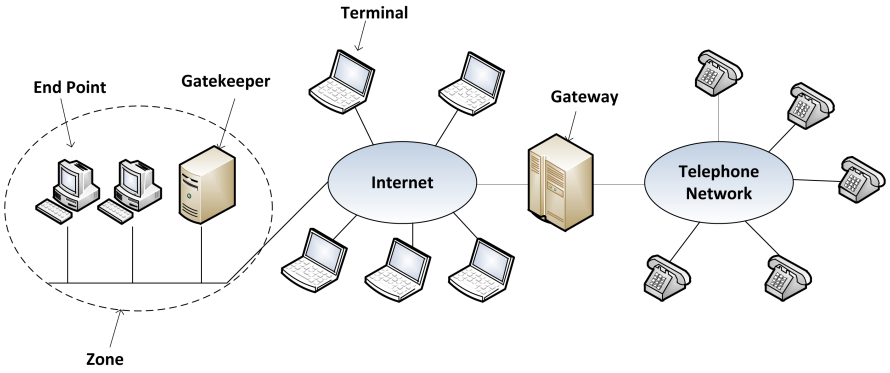

Figure A.1: H.323 General Model [TW10].

The H.323 approach leads to very well defined set of protocols for each layer, giving interoperability to a system. However, it is a complex and rigid standard which can be difficult to adapt to future applications [TW10].

Appendix B

SIP

The SIP protocol details how to set up Internet telephone calls, video conferences, and other multimedia connections. It just handles setup, management, and termination of sessions. A SIP protocol can establish ordinary telephone calls, multiparty sessions where everyone can hear and speak, and multicast sessions.

SIP protocol is a text-based protocol modeled on HyperText Transfer Protocol (HTTP). It uses messages in ASCII text to start a session. The text consists on a method name with additional lines containing headers, which some are taken from Multipurpose Internet Mail Extensions (MIME) to allow interworking with existing Internet applications. The entire process of initiation and termination of a session can be seen in Figure B.1.

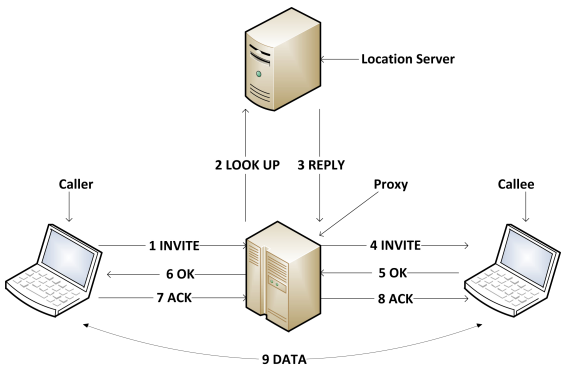

Figure B.1: SIP General Model [TW10].

SIP is an application-layer protocol that can run over UDP or TCP, as required. To initiate a session, the caller can create a TCP connection with the callee and send an INVITE message over it or send the INVITE message in a UDP packet.

It has the advantage of being a lightweight module that interworks well with other Internet protocols. Also, 3GPP has redefined the SIP protocol, which is currently used as the main protocol for several 3G and 4G network services. [TMM+07].

Appendix C

Analytical $n^{P^\star}$ and PER

P	E_b/N_0	n_0	n_1	n_2	PER (n_0)	PER (n_1)	PER (n_2)
1	12	1	1	1	0,3452	1,6e-05	1,0e-15
2	12	1	1	1	0,9999	0,0930	4,1e-07
3	12	2	1	1	0,9994	0,0269	1,6e-07
4	12	3	1	1	0,9624	0,0109	8,1e-09
5	12	3	1	1	0,9973	0,7939	0,0039
1	11	1	1	1	0,5957	0,0002	2,5e-12
2	11	1	1	1	0,9999	0,1722	2,0e-05
3	11	2	1	1	0,9995	0,0692	1,1e-06
4	11	3	1	1	0,9668	0,0289	4,3e-07
5	11	4	1	1	0,8146	0,0096	3,8e-08
1	10	1	1	1	0,8204	0,0027	4,2e-09
2	10	1	1	1	0,9999	0,3533	0,0003
3	10	2	1	1	0,9996	0,1294	2,1e-05
4	10	3	1	1	0,9710	0,0533	2,7e-06
5	10	4	1	1	0,8328	0,0246	8,2e-07

Table C.1: Theoretical data results (a) [VGaB$^+$13].

P	E_b/N_0	n_0	n_1	n_2	PER (n_0)	PER (n_1)	PER (n_2)
1	9	1	1	1	0,9456	0,0099	1,3e-07
2	9	1	1	1	0,9999	0,4858	0,0015
3	9	2	1	1	0,9997	0,2322	0,0002
4	9	3	1	1	0,9761	0,1054	4,3e-05
5	9	4	1	1	0,8537	0,0473	8,7e-06
1	8	1	1	1	0,9802	0,0306	5,2e-06
2	8	2	1	1	0,6953	0,0109	1,2e-06
3	8	2	1	1	0,9998	0,3671	0,0018
4	8	3	1	1	0,9809	0,1961	0,0003
5	8	4	1	1	0,8757	0,0951	0,0001
1	7	1	1	1	0,9982	0,1384	0,0003
2	7	2	1	1	0,8387	0,0405	3,1e-05
3	7	3	1	1	0,5297	0,0111	3,0e-06
4	7	3	1	1	0,9854	0,3031	0,0028
5	7	4	1	1	0,8962	0,1562	0,0006
1	6	2	1	1	0,3279	0,0050	1,46e-06
2	6	2	1	1	0,9356	0,1211	0,0005
3	6	3	1	1	0,6909	0,0429	0,0001
4	6	4	1	1	0,4608	0,0154	1,7e-05
5	6	5	1	1	0,2899	0,0053	3,2e-06
1	5	2	1	1	0,6438	0,0417	0,0002
2	5	3	1	1	0,2719	0,0062	7,3e-06
3	5	4	1	1	0,1478	0,0015	8,2e-07
4	5	4	1	1	0,6056	0,0477	0,0003
5	5	5	1	1	0,4092	0,0197	5,4e-05

Table C.2: Theoretical data results (b) [VGaB$^+$13].

P	E_b/N_0	n_0	n_1	n_2	PER (n_0)	PER (n_1)	PER (n_2)
1	4	3	1	1	0,1637	0,0027	4,3e-06
2	4	3	1	1	0,4789	0,0309	0,0002
3	4	4	1	1	0,2996	0,0110	4,2e-05
4	4	5	1	1	0,1776	0,0037	7,8e-06
5	4	5	2	1	0,5435	0,0075	1,1e-05
1	3	3	2	1	0,4059	0,0042	6,0e-06
2	3	4	1	1	0,1994	0,0061	2,8e-05
3	3	4	2	1	0,4701	0,0080	2,3e-05
4	3	5	2	1	0,3202	0,0028	3,7e-06
5	3	6	1	1	0,2212	0,0093	6,3e-05
1	2	4	2	1	0,2072	0,0021	4,2e-06
2	2	4	2	1	0,4032	0,0092	3,9e-05
3	2	4	2	2	0,6709	0,0369	8,2e-05
4	2	5	2	1	0,5063	0,0191	0,0002
5	2	5	2	2	0,7671	0,0794	0,0004
1	1	4	2	2	0,5047	0,0278	0,0001
2	1	4	2	2	0,6357	0,0497	0,0003
3	1	5	2	2	0,4544	0,0224	9,3e-05
4	1	5	2	2	0,6790	0,0697	0,0007
5	1	6	2	2	0,5195	0,0362	0,0002
1	0	5	2	2	0,4594	0,0364	0,0004
2	0	6	2	2	0,2355	0,0081	3,7e-05
3	0	6	2	2	0,3371	0,0181	0,0001
4	0	7	2	2	0,2387	0,0086	4,3e-05
5	0	7	3	2	0,3706	0,0091	3,1e-05

Table C.3: Theoretical data results (c) [VGaB$^+$13].

P	E_b/N_0	n_0	n_1	n_2	PER (n_0)	PER (n_1)	PER (n_2)
1	-1	6	3	3	0,4491	0,0223	9,4e-05
2	-1	6	3	3	0,4492	0,0231	0,0001
3	-1	6	3	3	0,5643	0,0387	0,0002
4	-1	7	3	3	0,4275	0,0203	8,9e-05
5	-1	7	3	3	0,5647	0,0442	0,0003
1	-2	8	3	3	0,3241	0,0171	0,0001
2	-2	8	3	3	0,2903	0,0127	8,3e-05
3	-2	8	3	3	0,3356	0,0185	0,0001
4	-2	8	4	3	0,4028	0,0150	7,6e-05
5	-2	9	3	3	0,3187	0,0172	0,0001
1	-3	9	4	4	0,4211	0,0274	0,0002
2	-3	9	4	4	0,3846	0,0221	0,0001
3	-3	9	4	4	0,3804	0,0209	0,0001
4	-3	9	4	4	0,4438	0,0307	0,0002
5	-3	10	4	4	0,3436	0,0172	0,0001
1	-4	11	5	5	0,4778	0,0343	0,0003
2	-4	11	5	5	0,3615	0,0191	0,0001
3	-4	10	5	5	0,4829	0,0379	0,0004
4	-4	11	5	5	0,3652	0,0201	0,0001
5	-4	11	5	5	0,4098	0,0247	0,0002

Table C.4: Theoretical data results (d) [VGaB$^+$13].

Bibliography

[AG11] MFL Abdullah and Mayada Faris Ghanim. An overview of CDMA techniques for mobile communications. *Journal of Mobile Communication*, 5(1):16–24, 2011.

[AMCV06] N. Anastacio, F. Merca, O. Cabral, and F.J. Velez. QoS metrics for cross-layer design and network planning for B3G systems. In *Wireless Communication Systems, 2006. ISWCS '06. 3rd International Symposium on*, pages 592–596, 2006.

[And05] J.G. Andrews. Interference cancellation for cellular systems: a contemporary overview. *Wireless Communications, IEEE*, 12(2):19–29, 2005.

[AR87] WS Adams and L Rider. Circular polar constellations providing continuous single or multiple coverage above a specified latitude. *Journal of the Astronautical Sciences*, 35:155–192, 1987.

[AS02] Tanenbaum Andrew S. *Computer Networks*. Prentice Hall, 4th edition, 2002.

[AUB99] Ian F. Akyildiz, Hüseyin Uzunalioğlu, and Michael D. Bender. Handover management in low earth orbit (LEO) satellite networks. *Mob. Netw. Appl.*, 4(4):301–310, December 1999.

[BCA12] Y. Bae, B. Choi, and A. Alfa. Achieving maximum throughput in random access protocols with multi-packet reception. *Mobile Computing, IEEE Transactions*, 2012.

[BCRS02] F Beritelli, S Casale, G Ruggeri, and S Serrano. Performance evaluation and comparison of G.729/AMR/fuzzy voice activity detectors. *Signal processing letters, IEEE*, 9(3):85–88, 2002.

[BCW96] R.M. Buehrer, N.S. Correal, and B.D. Woerner. A comparison of multiuser receivers for cellular CDMA. In *Global Telecommunications Conference, 1996. GLOBECOM '96. 'Communications: The Key to Global Prosperity*, volume 3, pages 1571–1577 vol.3, 1996.

[BNNK08] A.M. Baker, Chee Kyun Ng, N.K. Noordin, and S. Khatun. PHY and MAC, cross-layer optimization and design. *In 6th National Conference on Telecommunication Technologies 2008 and 2nd Malaysia Conference on Photonics 2008*, Putrajaya, Malaysia, August 2008.

[BS04] Ahmad R.S. Bahai and Burton R. Saltzberg. *Multi-carrier Digital Communications Theory and Applications of OFDM*. Springer Verlag, New York, 2004.

[BWZ00] D.J. Bem, T.W. Wieckowski, and R.J. Zielinski. Broadband satellite systems. *Communications Surveys Tutorials, IEEE*, 3(1):2–15, 2000.

[CC84] R. Comroe and Jr. Costello, D.J. ARQ schemes for data transmission in mobile radio systems. *Selected Areas in Communications, IEEE Journal on*, 2(4):472–481, 1984.

[CD01] Mainak Chatterjee and Sajal K Das. Performance evaluation of a request-TDMA/CDMA protocol for wireless networks. *Journal of Interconnection Networks*, 2(01):49–67, 2001.

[CF07] D.J. Costello and Jr. Forney, G.D. Channel coding: The road to channel capacity. *Proceedings of the IEEE*, 95(6):1150–1177, 2007.

[CR12] Barry R. Cobb and Rafael Rumí. Approximating the distribution of a sum of log-normal random variables. *Wireless Communications, IEEE Transactions*, Granada, Spain, 2012.

[DMB+09] R. Dinis, P. Montezuma, L. Bernardo, R. Oliveira, M. Pereira, and P. Pinto. Frequency-domain multipacket detection: a high throughput technique for SC-FDE systems. *Wireless Communications, IEEE Transactions on*, 8(7):3798–3807, 2009.

[DSM04] Trang Dinh Dang, B. Sonkoly, and S. Molnar. Fractal analysis and modeling of VoIP traffic. In *Telecommunications Network Strategy and Planning Symposium. NETWORKS 2004, 11th International*, pages 123–130, 2004.

[FABSE02] D. Falconer, S.L. Ariyavisitakul, A. Benyamin-Seeyar, and B. Eidson. Frequency domain equalization for single-carrier broadband wireless systems. *Communications Magazine, IEEE*, 40(4):58–66, 2002.

[Fel96] Phillip M. Feldman. *An Overview and Comparison of Demand Assignment Multiple Access (DAMA) Concepts for Satellite Communications Networks. DTIC Document*, Rand Publishing, November 1996.

[GaBD+12] F. Ganhão, L. Bernardo, R. Dinis, G. Barros, E. Santos, A. Furtado, R. Oliveira, and P. Pinto. Energy-efficient QoS provisioning in demand assigned satellite NDMA schemes. In *Computer Communications and Networks (ICCCN), 2012 21st International Conference on*, pages 1–8, 2012.

[GaDB+11] F. Ganhão, R. Dinis, L. Bernardo, P. Carvalho, R. Oliveira, and P. Pinto. Analytical performance evaluation of SC-FDE modulations with packet combining and multipacket detection schemes. In *Vehicular Technology Conference (VTC Spring), 2011 IEEE 73rd*, pages 1–5, 2011.

[GaPB+11] Francisco Ganhão, Miguel P. Pereira, Luis Bernardo, Rui Dinis, Rodolfo Oliveira, and Paulo Pinto. Performance of hybrid ARQ for NDMA access schemes with uniform average power control. *JCM*, 6(9):691–699, 2011.

[GL00] Ajay Chandra V Gummalla and John O. Limb. Wireless medium access control protocols. *Communications Surveys Tutorials, IEEE*, 3(2):2–15, 2000.

[GL08] Fredrik Gustafson and Marcus Lindahl. *Evaluation of Stastical Distributions for VoIP Traffic Modelling.* PhD Thesis. University West, Department of Economics and IT, May 2008.

[GLASW07] J.J. Garcia-Luna-Aceves, Hamid R. Sadjadpour, and Zheng Wang. Challenges: towards truly scalable ad-hoc networks. *Proceedings of the 13th annual ACM international conference on Mobile computing and networking*, Montreal, Canada, 2007.

[Har01] William C. Hardy. *QoS: Measurement and Evaluation of Telecommunications Quality of Service.* John Wiley & Sons, Inc., New York, NY, USA, 2001.

[HKL97] B. Hajek, A. Krishna, and Richard O. LaMaire. On the capture probability for a large number of stations. *Communications, IEEE Transactions on*, 45(2):254–260, 1997.

[HL01] Yurong Hu and V.O.K. Li. Satellite-based internet: a tutorial. *Communications Magazine, IEEE*, 39(3):154–162, 2001.

[HLZ08] Wei Lan Huang, Khaled Letaief, and Ying Zhang. Cross-layer multi-packet reception based medium access control and resource allocation for space-time coded MIMO/OFDM. *Wireless Communications, IEEE Transactions on*, 7(9):3372–3384, 2008.

[Hor13] Kurt Hornik. Exploring heavy tails pareto and generalized pareto distributions. Technical Report. Institute for Statistics and Mathematics, Wien, January 2013.

[Ipp08] Louis J. Ippolito. *Satellite Communications Systems Engineering: Atmospheric Effects, Satellite Link Design and System Performance (Wireless Communications and Mobile Computing).* Wiley Publishing, 2008.

[Lar78] Simon S Lara. An analysis of the reservation-aloha protocol for satellite packet switching. *Conference Rec. International Conference on Communications*, Toronto, June 1978.

[LB05] Stephen W Laverty and Donald R Brown. Improved voice activity detection in the presence of passing vehicle noise. *Technical Report. Worcester Polytechnic Institute*, 2005.

[LCM84] Shu Lin, D. Costello, and M. Miller. Automatic-repeat-request error-control schemes. *Communications Magazine, IEEE*, 22(12):5–17, 1984.

[LPW09] David Asher Levin, Yuval Peres, and Elizabeth Lee Wilmer. *Markov chains and mixing times*. AMS Bookstore, 2009.

[LSW12] Jia-Liang Lu, Wei Shu, and Min-You Wu. A survey on multipacket reception for wireless random access networks. *Journal of Computer Networks and Communications*, 2012.

[LV89] R. Lupas and S. Verdu. Linear multiuser detectors for synchronous code-division multiple-access channels. *Information Theory, IEEE Transactions on*, 35(1):123–136, 1989.

[LV90] R. Lupas and S. Verdu. Near-far resistance of multiuser detectors in asynchronous channels. *Communications, IEEE Transactions on*, 38(4):496–508, 1990.

[Man95] T.E. Mangir. The future of public satellite communications. In *In 1995 IEEE Aerospace Applications Conference, (AEROCONF 1995), Aspen, USA*, pages 393–410 vol.1, 1995.

[Maz99] S Mazur. A description of current and planned location strategies within the orbcomm network. *International journal of satellite communications*, 17(4):209–223, 1999.

[MV05] M. Madueno and J. Vidal. Joint physical-mac layer design of the broadcast protocol in ad hoc networks. *Selected Areas in Communications, IEEE Journal on*, 23(1):65–75, 2005.

[NBSL11] Narayanan Natarajan, A. Bagchi, W.E. Stephens, and S.J. Leanheart. Network architecture for mission critical communications using LEO satellites. In

MILITARY COMMUNICATIONS CONFERENCE, 2011 - MILCOM 2011, pages 2087–2092, 2011.

[NGN+07] A. Nassery, M.R. Ghajar, S. Najafzadeh, M.A. Khajehnejad, and B. Forouzandeh. Evaluation of hardware/software partitioning of conjugate-structure algebraic celp (cs-acelp) algorithm using matlab. In *Information and Communication Technology, 2007. ICICT '07. International Conference on*, pages 287–290, 2007.

[PA02] E.L. Pinto and C.P. Albuquerque. A técnica de transmissão OFDM. *Revista Científica*, 2002.

[PBD+13] M Pereira, L Bernardo, R Dinis, R Oliveira, and P Pinto. On the use of frequency-domain cross-layer diversity techniques to cope with lost packets. *Physical Communication*, 2013.

[Pey99] H. Peyravi. Medium access control protocols performance in satellite communications. *Communications Magazine, IEEE*, 37(3):62–71, 1999.

[PRFT99] S.R. Pratt, R.A. Raines, C.E. Fossa, and Michael A. Temple. An operational and performance overview of the iridium low earth orbit satellite system. *Communications Surveys Tutorials, IEEE*, 2(2):2–10, 1999.

[Rap01] Theodore Rappaport. *Wireless Communications: Principles and Practice*. Prentice Hall PTR, Upper Saddle River, NJ, USA, 2nd edition, 2001.

[Ret80] C. Retnadhas. Satellite multiple access protocols. *Communications Magazine, IEEE*, 18(5):16–20, 1980.

[RP12] R. Ramya and S. Padmapriya. Multi packet reception technique with MIMO assisted cross layered MAC/PHY algorithm over a jittery channel. *International Journal of Research in Communication Technologies*, 1(1), 2012.

[SBT11] S. Sesia, M. Baker, and I. Toufik. *LTE - The UMTS Long Term Evolution: From Theory to Practice*. John Wiley and Sons, 2011.

[SCJ11] R. Stankiewicz, P. Cholda, and A. Jajszczyk. Qox: What is it really? *Communications Magazine, IEEE*, 49(4):148–158, 2011.

[Sha48] Claude E. Shannon. A mathematical theory of communication. *The Bell System Technical Journal*, 27:379–423, 623–656, July, October 1948.

[SRGM07] R. Samano-Robles, M. Ghogho, and D.C. McLernon. Quality of service in wireless network diversity multiple access protocols based on a virtual time-slot allocation. In *Communications, 2007. ICC '07. IEEE International Conference on*, pages 5843–5848, 2007.

[TMM+07] G. Thanos, A. Meliones, M. Marinidou, E. de la Fuente, and G. Konstantoulakis. A 3GPP-SIP media gateway for the ip multimedia subsystem. In *Software, Telecommunications and Computer Networks, 2007. SoftCOM 2007. 15th International Conference on*, pages 1–5, 2007.

[TO00] S.G. Tanyer and H. Ozer. Voice activity detection in nonstationary noise. *Speech and Audio Processing, IEEE Transactions*, 8(4):478–482, 2000.

[TV09] David N. C. Tse and Pramod Viswanath. Fundamentals of wireless communication. *IEEE Transactions on Information Theory*, 55(2):919–920, 2009.

[TW10] Andrew S. Tanenbaum and David J. Wetherall. *Computer Networks*. Prentice Hall, 5th edition, October 2010.

[TZB00] M.K. Tsatsanis, Ruifeng Zhang, and S. Banerjee. Network-assisted diversity for random access wireless networks. *Signal Processing, IEEE Transactions*, 48(3):702–711, 2000.

[Uni02] International Telecommunications Union. Itu handbook on satellite communications. Wiley-Interscience, 2002.

[VGaB+13] J. Vieira, F. Ganhão, L. Bernardo, R. Dinis, M. Beko, R. Oliveira, and P. Pinto. Random access ndma mac protocols for satellite networks. *Internet of Things, Smart Spaces, and Next Generation Networking*, Springer Berlin Heidelberg. pages 427–438, 2013.

[WGLA09] Xin Wang and JJ Garcia-Luna-Aceves. Embracing interference in ad hoc networks using joint routing and scheduling with multiple packet reception. *Ad Hoc Networks*, 7(2):460–471, 2009.

[Wic95] Stephen B. Wicker. *Error Control Systems for Digital Communication and Storage*. Prentice-Hall, Upper Saddle River, NJ, USA, 1995.

[XSR90] Zhenhua Xie, R.T. Short, and C.K. Rushforth. A family of suboptimum detectors for coherent multiuser communications. *Selected Areas in Communications, IEEE Journal on*, 8(4):683–690, 1990.

[ZR94] M. Zorzi and R.R. Rao. Capture and retransmission control in mobile radio. *Selected Areas in Communications, IEEE Journal on*, 12(8):1289–1298, 1994.

[ZST99] Ruifeng Zhang, N.D. Sidiropoulos, and M.K. Tsatsanis. Collision resolution in packet radio networks using rotational invariance techniques. In *Global Telecommunications Conference, 1999. GLOBECOM '99*, volume 1B, pages 667–671 vol. 1b, 1999.

[ZT02] Ruifeng Zhang and Michail K Tsatsanis. Network-assisted diversity multiple access in dispersive channels. *Communications, IEEE Transactions on*, 50(4):623–632, 2002.